

# 4.2.2.2

## Enhanced Internal Cooling of Turbine Blades and Vanes



Je-Chin Han



Lesley M. Wright

Turbine Heat Transfer Laboratory  
Department of Mechanical  
Engineering  
Texas A&M University  
College Station, Texas 77843-3123,  
USA

email: jc-han@tamu.edu

### 4.2.2.2-1 Introduction

Gas turbines play a vital role in the today's industrialized society, and as the demands for power increase, the power output and thermal efficiency of gas turbines must also increase. One method of increasing both the power output and thermal efficiency of the engine is to increase the temperature of the gas entering the turbine. In the advanced gas turbines of today, the turbine inlet temperature can be as high as 1500°C; however, this temperature exceeds the melting temperature of the metal airfoils. Therefore, it is imperative that the blades and vanes are cooled, so they can withstand these extreme temperatures. Cooling air around 650°C is extracted from the compressor and passes through the airfoils. With the hot gases and cooling air, the temperature of the blades can be lowered to approximately 1000°C, which is permissible for reliable operation of the engine.

It is widely accepted that the life of a turbine blade can be reduced by half if the temperature prediction of the metal blade is off by only 30°C. In order to avoid premature failure, designers must accurately predict the local heat transfer coefficients and local airfoil metal temperatures. By preventing local hot spots, the life of the turbine blades and vanes will increase. However, due to the complex flow around the airfoils it is difficult for designers to accurately predict the metal temperature. Figure 1 shows the heat flux distribution around an inlet guide vane and a rotor blade. At the leading edge of the vane, the heat transfer coefficients are very high, and as the flow splits and travels along the vane, the heat flux decreases. Along the suction side of the vane, the flow transitions from laminar to turbulent, and the heat transfer coefficients increase. As the flow accelerates along the pressure surface, the heat transfer coefficients also increase. The trends are similar for the turbine blade: the heat flux at the leading edge is very high and continues decrease as the flow travels along the blade; on the suction surface, the flow transitions from laminar to turbulent, and the heat flux sharply increases; the heat transfer on the pressure surface increases as the flow accelerates around the blade.

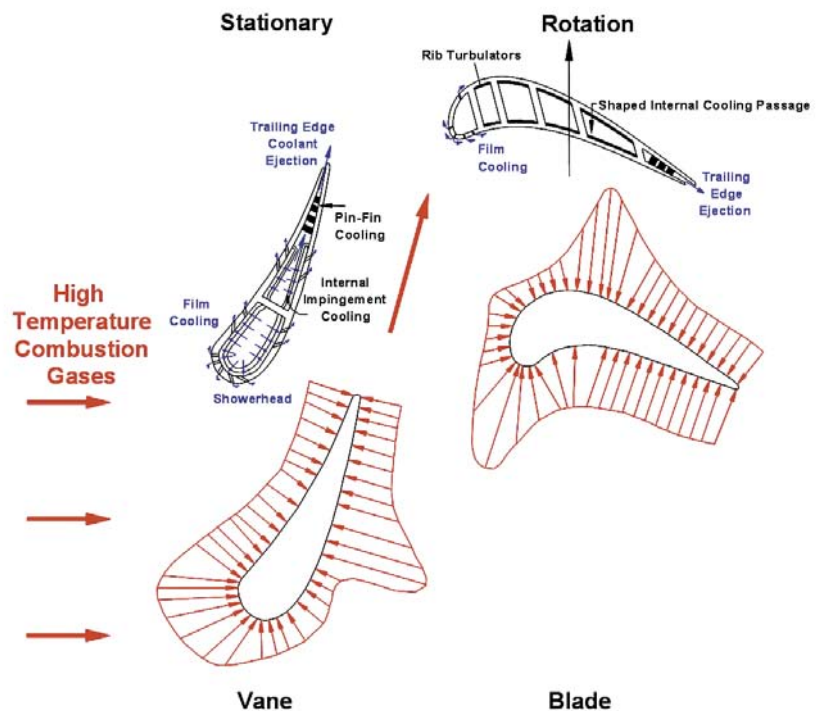


Fig. 1. Cross-Sectional View and Heat Flux Distribution of a Cooled Vane and Blade

Due to the complex flow, designers need data that will aid them in the development of efficient cooling designs. They need detailed hot gas path heat transfer distributions. Heat transfer and film cooling data are also needed for the airfoils. The surface heat transfer on a stator vane is affected by the combustor-generated high turbulence, the laminar-to-turbulent transition, acceleration, film cooling flow, platform secondary flow, and surface roughness. These factors as well as the rotational, centrifugal forces and blade tip clearance and leakage must be considered for the rotating blades.

After the potential hot spots on the airfoil surface are identified, the internal cooling schemes can be developed. Designers need new internal heat transfer data to improve current rotor blade cooling performance. They also need detailed flow and heat transfer data to understand the flow physics and to improve the current internal cooling designs. Many techniques have been developed to enhance the heat transfer in these passages. The cooling passages located in the middle of the airfoils are often lined with rib turbulators. Near the leading edge of the blade, jet impingement (coupled with film cooling) is commonly used. Jet impingement is also used throughout the cross-section of the stator vanes. Pin-fins and dimples can be used in the trailing edge portion of the vanes and blades. These techniques have also been combined to further increase the heat transfer from the airfoil walls.

A number of traditional cooling concepts are used in various combinations to adequately cool the turbine vanes and blades; these techniques are identified and described throughout this chapter. In addition, newly developed, advanced cooling concepts are also introduced as possible cooling alternatives. The interested reader is referred to *Gas Turbine Heat Transfer and Cooling Technology* by Han et al. for a more in depth description of turbine blade heat transfer and cooling<sup>1</sup>. In addition, Lakshminarayana reviewed recent publications involving turbine cooling and heat transfer, and Dunn put together a detailed review of convective heat transfer and aerodynamics in axial flow turbines<sup>2</sup>. A symposium volume discussing heat transfer in gas turbine systems is also available by Goldstein<sup>3</sup>.

#### 4.2.2.2-2 Enhanced Internal Cooling of Turbine Vanes

A typical cooled turbine vane is shown in figure 2. As shown in the figure, the vane is hollow, so cooling air can pass through the vane internally. The coolant is extracted from the internal channel for impingement and pin-fin cooling. Jet impingement is a very aggressive cooling technique which very effectively removes heat from the vane wall. However, this technique is not readily applied to the narrow trailing edge. The vane trailing edge is cooled using pin-fins (an array of short cylinders). The pin-fins increase the heat transfer area while effectively mixing the coolant air to lower the wall temperature of the vanes. After impinging on the walls of the airfoil, the coolant exits the vane and provides a protective film on the vane's external surface. Similarly, the coolant traveling through the pin-fin array is ejected from the trailing edge of the airfoil.

##### *Impingement Cooling*

Impingement cooling is commonly used near the leading edge of the airfoils, where the heat loads are the greatest. With the cooling jets striking (impinging) the blade wall, the leading edge is well suited for impingement cooling because of the relatively thick blade wall in this area. Impingement can also be used near the mid-chord of the vane. Figure 2 shows jet impingement located throughout the cross-section of an inlet guide vane. Several aspects must be considered when developing efficient cooling designs. The effect of jet-hole size and distribution, cooling channel cross-section, and target surface shape all have significant effects on the heat transfer coefficient distribution. Jet impingement near the mid-chord of the blade is very similar to impingement on a flat plate; however, the sharp curvature at the leading edge of the vane must be considered when utilizing impingement in this region.

##### *Jet Impingement from Multiple Jets*

As shown in figure 2, many jets are used to increase the heat transfer from the vane wall. It has been shown by Metzger et al. that multiple jets perform very differently from a single jet striking a target surface<sup>4</sup>. They concluded that for multiple jets, the Nusselt number is strongly dependent on the Reynolds number, while there is no significant dependence on the jet-to-target plate spacing.

The difference is due to the jet cross-flow from the spent jets. Studies by Florschuetz et al. and Koopman and Sparrow showed that the mass from one jet moves in the cross-jet flow direction, and this flow can alter the performance of neighboring jets<sup>5</sup>. The cross-flow attempts to deflect a jet away from its impinging location on the target plate. In situations with very strong cross-flow and sufficiently

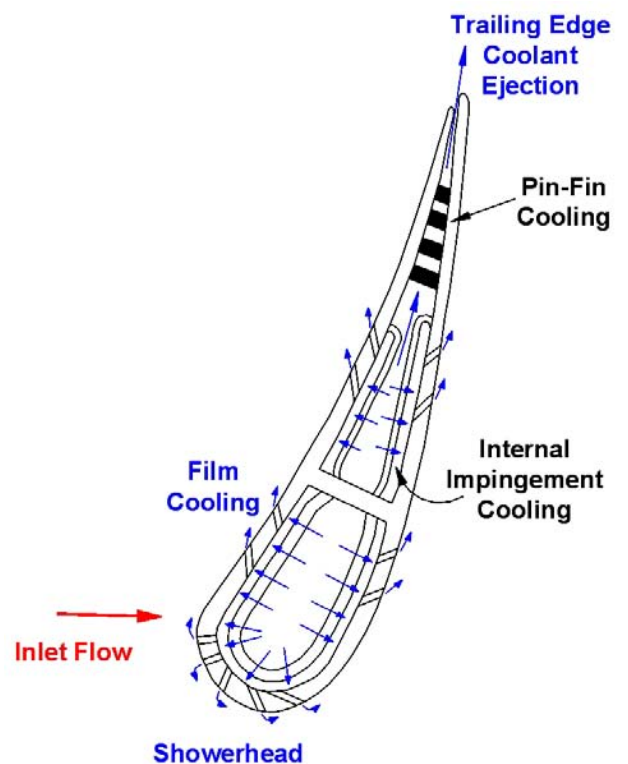


Fig. 2. Schematic of a Turbine Vane Cross-Section with Impingement and Trailing Edge Pin-Fin Cooling

large jet-to-target plate spacing, the cross-flow can completely deflect the jet away from the impingement surface. Florschuetz and Su reported that cross-flow decreases the overall heat transfer from the impingement surface<sup>6</sup>. They determined that cross-flow enhances the convective heat transfer, but the enhancement from the jets decreases, as the jets are deflected. Because the enhancement from the impingement jets is much greater than the convective enhancement, the overall Nusselt numbers decrease in the presence of cross-flow. A typical test model used by Florschuetz et al. is shown in figure 3<sup>7</sup>. As shown in this figure, the coolant jets impinge on the target surface from the jet plate in an in-line array. As the coolant travels along the test surface, the spent air from the upstream jets effects the heat transfer coefficient distributions of the downstream jets, and this effect increases as more spent air accumulates on the target surface.

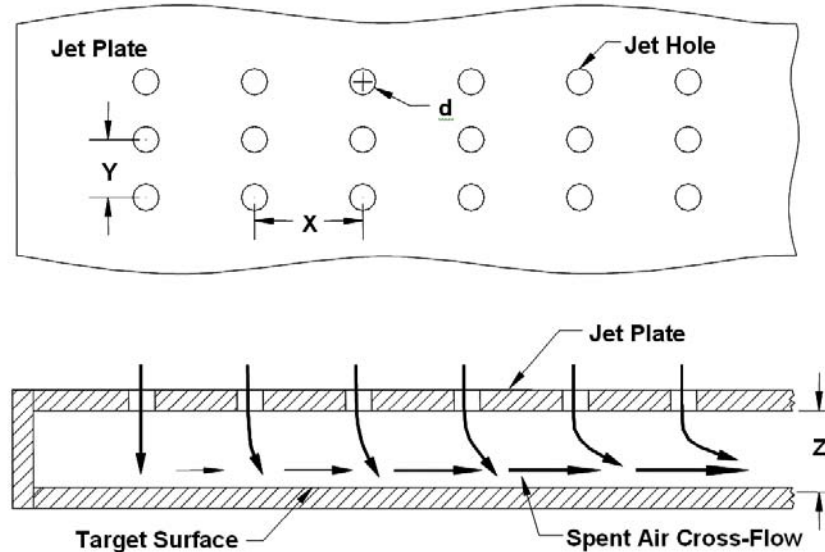


Fig. 3. A Typical Test Model for Impingement Cooling Studies

Correlations based on experimental data were developed by Kercher and Tabakoff and Florschuetz et al. to estimate the heat transfer enhancement from an array of impinging jets<sup>8</sup>. Although the correlations are in different forms, they both demonstrate the dependence of the heat transfer enhancement on the amount of cross-flow. Florschuetz et al. also showed the cross-flow effect is much stronger in staggered arrays of jets than an in-line array<sup>9</sup>. Bailey and Bunker extended the correlation developed by Florschuetz et al. to include the effect of jet spacing<sup>10</sup>. The correlation has been extended to include dense impingement arrays.

Huang et al. controlled the direction of the cross-flow and obtained detailed distributions of the heat transfer coefficients for three target plates<sup>11</sup>. Their results clearly indicate when the cross-flow travels in two opposite directions, the heat transfer enhancement on the target plate is much greater than when the cross-flow is restricted to one direction. This study was extended by Ekkad et al. to include the effect of coolant extraction for film cooling<sup>12</sup>. The heat transfer enhancement on the target plate decreases near the edges due to the decreased coolant flow (for film cooling). Wang et al. investigated cross-flow through a confined space; they also considered cross-flow traveling in one direction and two directions<sup>13</sup>. This study also concluded that increasing cross-flow results in degraded heat transfer; however, the heat transfer coefficient distribution is much more uniform.

The heat transfer coefficient distributions on target plates with stretched arrays of impinging jets were studied by Gao et al.<sup>14</sup>. This array varies from the traditional square array in which the jets are evenly spaced. They concluded the existing correlations for square arrays over-predict the effect of cross-flow in the target surface.

The presence of initial cross-flow also effects the heat transfer enhancement from the target plate. The cross-flow described above is created by the spent flow from the jets. Therefore, the first row of jets is not affected by the cross-flow. However, in many situations, cross-flow may develop upstream of the first row. The flow from upstream of the impingement jets can significantly alter the flow near the jets, and thus alter the heat transfer coefficients on the target surface. Florschuetz et al. investigated the effect of initial cross-flow on the heat transfer enhancement<sup>15</sup>. The results of this study were similar to those mentioned above describing cross-flow: the heat transfer enhancement on the target plate decreases when initial cross-flow is present.

### *Jet Impingement on a Curved Surface*

The above studies investigated the heat transfer on flat target plates. The results obtained for flat plates can be applied to impingement near the mid-chord of the blade. However, the effect of target surface curvature must be considered when implementing jet impingement near the leading edge of the airfoil. The curvature of the airfoil creates different cross-flow behavior, and therefore, the heat transfer coefficients on the curved surface are different than those on the flat surface. Chupp et al. studied impingement on a curved surface, and this group concluded that the average Nusselt number ratio increases as the curvature of the target plate increases<sup>16</sup>. The effect of target surface shape was also pursued by Bunker and Metzger<sup>17</sup>. They concluded that a sharper nose radius yields a more

## 4.2.2.2 Enhanced Internal Cooling of Turbine Blades and Vanes

uniform Nusselt number distribution compared to a smooth-nosed chamber. This study was also extended to include the effect of coolant extraction for film cooling<sup>18</sup>. When the bleed from the pressure and suction surfaces is equal, the greatest reduction in the Nusselt numbers occurs.

### *Pin-Fin Cooling*

Due to manufacturing constraints in the very narrow trailing edge of the blade, pin-fin cooling is typically used to enhance the heat transfer from the blade wall in this region. The pins typically have a height-to-diameter ratio between  $\frac{1}{2}$  and 4. In a pin-fin array heat is transferred from both the smooth channel endwall and the numerous pins. Flow around the pins in the array is comparable to flow around a single cylinder. As the coolant flows past the pin, the flow separates and wakes are shed downstream of the pin. In addition to this wake formation, a horseshoe vortex forms just upstream of the base of the pin, and the vortex wraps around the pins. This horseshoe vortex creates additional mixing, and thus enhanced heat transfer.

Many factors must be considered when investigating pin-fin cooling. The type of pin-fin array and the spacing of the pins in the array effect the heat transfer distribution in the channel. The pin size and shape also have a profound impact on the heat transfer in the cooling passage. Because pin-fins are commonly coupled with trailing edge ejection (as shown in figure 2), the effect of this coolant extraction must also be considered.

### *Pin Array and Partial Length Pin Arrangement*

There are two array structures commonly used. One is the inline array and the other is the staggered array. Figure 4 shows a typical experimental test model with a staggered array of pin-fins. Metzger et al. used staggered arrays of circular pins with 1.5 to 5 pin diameter spacing in a rectangular channel<sup>19</sup>. A closer spaced array (smaller  $x/D$ ) shows a higher heat transfer coefficient. Their observations clearly indicate that addition of pin-fins significantly enhances the heat transfer coefficient. However, the addition of pins also increases the pressure drop in the flow channel. Chyu et al. showed that the heat transfer coefficient on the pin surface for both arrays is consistently higher than that of the channel endwall<sup>20</sup>. The pin surface heat transfer is observed to be 10 to 20 percent higher for the presented case. Experimental results have been correlated by Metzger et al. and VanFossen to predict the Nusselt number in channels with pin-fin arrays<sup>21</sup>. The average Nusselt number in a channel with short pin-fins is primarily dependent on the Reynolds number of the flow, and a weaker dependence is shown for the pin spacing.

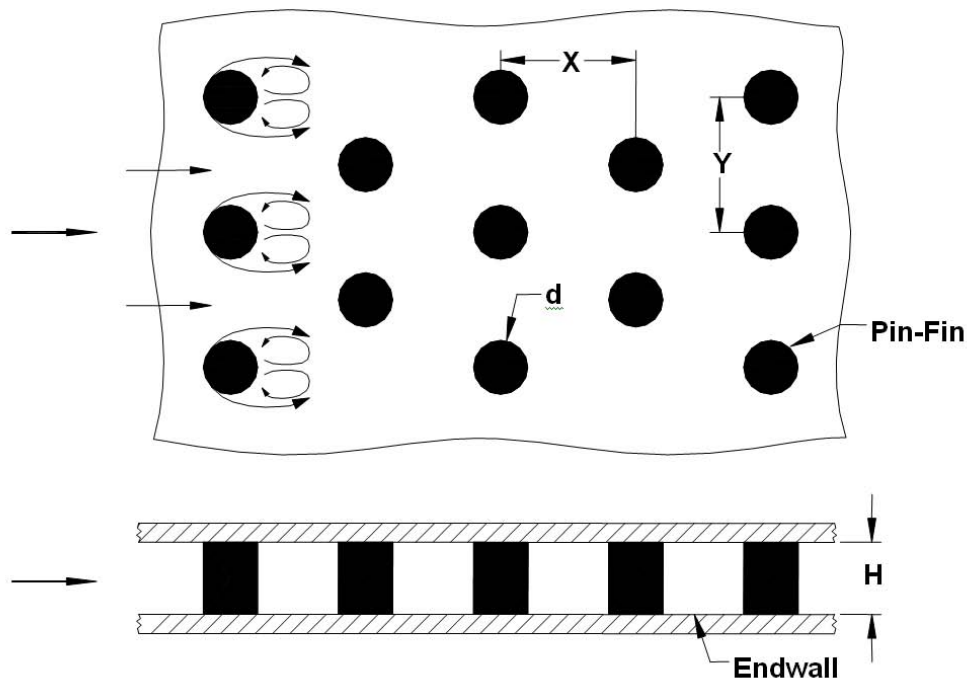


Fig. 4. A Typical Test Model and Secondary Flow for Pin-Fin Cooling Studies

Arora and Abdel-Messeh studied the effects of partial length pins in a rectangular channel<sup>22</sup>. The surface containing pins is not affected by the pin tip clearance. Whereas the opposite surface, that does not have pins, shows a decrease in heat transfer coefficient with an increase in the pin tip clearance. The friction factor is lower for partial pins compared to full-length pins. In general, the heat transfer coefficient decreases with partial length pins.

### *Effect of Pin Shape and Array Orientation*

Metzger et al. studied the effects of pin shape and array orientations<sup>23</sup>. They reported the effect of flow incident angle on oblong pins. All incident angles except 90° yield higher Nusselt numbers than circular pins. The  $\gamma = 90^\circ$  array yields significantly lower Nusselt numbers, especially toward the lower end of the Reynolds number range. The  $\gamma = \pm 30^\circ$  array has the highest Nusselt numbers, about 20 percent higher than the circular pin array on the average. Except for  $\gamma = 90^\circ$ , the pressure drop for oblong pins are significantly higher than circular pins. This increase in the friction factor is associated with the flow turning caused by oblong pins. The pin shapes mostly studied are straight cylinders. However, the casting or other manufacturing processes cannot make perfect cylinders and these manufacturing imperfections may affect the heat transfer performance.

Chyu studied the effect of a fillet at the base of the cylindrical pin<sup>24</sup>. Straight cylinders in staggered array formation have the highest heat transfer followed by filleted cylinders in the staggered formation. It is interesting to note that the fillet cylinder inline formation has better heat transfer than the straight cylinders in the inline formation. Though a staggered array gives higher heat transfer coefficients, performance of the inline straight cylinders is best among the group and the fillet cylinders in staggered formation are the worst. In a different experimental work, Goldstein et al. studied the effect of stepped diameters on mass transfer coefficients<sup>25</sup>. The diameter of the pin is axially varied. The base diameter is greater than the center diameter and no fillet radius is provided. The array configuration is staggered. Results show that the mass transfer increases or remains the same compared to a straight cylinder pin array when the radius is varied, but the pressure drop reduces significantly for the stepped diameter cylindrical pins.

Chyu et al. used cube and diamond shaped pins to enhance the heat transfer coefficient from a surface<sup>26</sup>. The cube-shaped pins have the highest mass transfer coefficients among the shapes considered and round pins have the lowest mass transfer coefficients. Corresponding pressure loss coefficients are higher for the cube and diamond shaped pins relative to the circular pins.

### *Effect of Flow Convergence and Turning*

The flow channel in the trailing edge of an airfoil has a reducing cross-section, and therefore, the flow in the channel accelerates. The results are row averaged and the accelerating flow shows an increase in the heat transfer coefficient<sup>27</sup>. Chyu et al. used mass transfer technique to study the effect of perpendicular flow entry in two pin-fin configurations<sup>28</sup>. They show that the turning inlet configuration always results in lower average Sherwood numbers. The reduction is about 40-50% for the inline array and 20-30% for the staggered array.

### *Pin-Fin Cooling With Ejection*

The trailing edge pin-fin channel normally has ejection holes through which the spent coolant exhausts to the main stream flow. Kumran et al. investigated the effects of the length of coolant ejection holes on the heat transfer coefficient in pin-fins<sup>29</sup>. The length of the ejection hole can significantly alter the discharge rate of coolant. More coolant ejection reduces the Nusselt number significantly from no ejection. This decrease in the heat transfer coefficient can be explained by the fact that coolant mass is extracted from the coolant channel before its cooling capacity is fully utilized. Results indicate that the correlation based on the local Reynolds number can predict the heat transfer coefficient distribution for lower coolant ejection but does not adequately predict the heat transfer coefficients at higher ejection rates. Hwang and Lu investigated a converging channel with ejection<sup>30</sup>. They also found that increasing the ejection degrades the endwall heat transfer near the tall wall opposite of the ejection, and the heat transfer on the channel endwall surface near the ejection holes is increased. They also concluded that square, diamond, and circular pin-fin arrays enhance the heat transfer equally in channels with large ejection flows.

### *Dimple Cooling*

In recent years, dimples have been considered as an alternative to pin-fin cooling. Dimpled cooling is a very desirable alternative due to the relatively low pressure loss penalty (compared with pins) and moderate heat transfer enhancement. A typical test section for dimple cooling studies is shown in figure 5; this figure also shows the dimple induced secondary flow. These concave dimples induce flow separation and reattachment with pairs of vortices. The areas of high heat transfer include the areas of flow reattachment on the flat surface immediately downstream of the dimple. The heat transfer in the dimpled channel is typically 2 to 2.5 times greater than the heat transfer in a smooth channel with a pressure loss penalty of 2 to 4 times that of a smooth channel. These values show little dependence on Reynolds number and channel aspect ratio. However, the dimple size, dimple depth (depth-to-print diameter ratio = 0.1 to 0.3), distribution, and shape (cylindrical, hemispheric, teardrop) each effect the heat transfer distribution in the channel. Recent studies have investigated the influence of these factors on the heat transfer in rectangular channels<sup>31</sup>. Dimples have also been investigated in a circular channel and similar levels of heat transfer enhancement and frictional losses were measured<sup>32</sup>.

Syred et al. compared the heat transfer enhancement due a single dimple on both flat and curved surfaces<sup>33</sup>. From this study it was shown that the surface curvature significantly influences the heat transfer enhancement. The heat transfer is further enhanced on a surface that is concavely shaped (compared to a flat surface); however, a convexly curved surface with a dimple decreases the level of heat transfer enhancement.

## 4.2.2.2 Enhanced Internal Cooling of Turbine Blades and Vanes

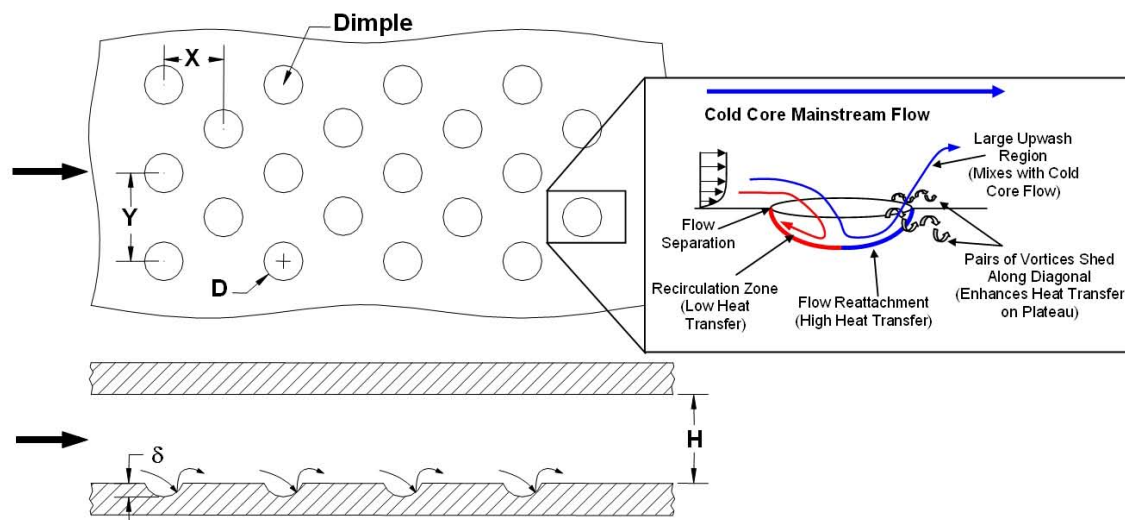


Fig. 5. A Typical Test Model for Dimple Cooling Studies with a Conceptual View of Dimple Induced Secondary Flow

### *Compound and New Cooling Techniques*

Several internal heat transfer enhancement techniques are discussed in previous sections. Most common methods of heat transfer augmentation in gas turbine airfoils are ribs, pins, and jet impingement. It is shown that these enhancement techniques increase heat transfer coefficients, but can combining these techniques increase the heat transfer coefficient more? Several researchers have combined these heat transfer enhancement techniques to improve the heat transfer coefficient. However, it is not always recommended to combine more than one heat transfer augmentation technique. In addition to compounding more than one heat transfer enhancement technique, there are attempts to incorporate new concepts (e.g., jet swirlers and heat pipes) in the turbomachinery cooling. An introduction of several new cooling techniques with their applications is presented here.

### *Impingement on Ribbed, Pinned, and Dimpled Walls*

Azad et al. studied the impingement effect on dimpled and pinned surfaces<sup>34</sup>. Because the dimples and pins are circular depressions and protrusions, respectively, these two target surfaces offer an interesting comparison of the heat transfer enhancement. At lower Reynolds number the pinned surface performs better than the dimpled surface. At higher Reynolds numbers, the dimpled surface performs better than the pinned surface for a certain flow orientation. Taslim et al. reported a significant increase in the heat transfer enhancement on a curved target surface roughened with conical bumps<sup>35</sup>. This study was extended to include film cooling holes, similar to the showerhead-type film cooling on the leading edge<sup>36</sup>. They concluded that the presence of leading edge extraction also significantly increases the heat transfer on the target surface. The heat transfer is further increased if the “racetrack” jet holes are used rather than traditional round jet holes<sup>37</sup>

### *Combined Effect of Swirl and Impingement*

A new jet impingement and swirl technique was investigated by Glezer et al.<sup>38</sup>. A preliminary test showed significant improvement in the heat transfer performance. Based on that study, a new airfoil has been designed with swirling impingement in the leading edge. This new airfoil is tested in a hot cascade test section. Results indicate that screw shaped swirl cooling can significantly improve the heat transfer coefficient over a smooth channel and this improvement is not significantly dependent on the temperature ratio and rotational forces. Moreover, it was concluded that optimization of the internal passage geometry in relation to location and size of the tangential slots is very important in achieving the best performance of the screw-shaped swirl in the leading edge cooling. Pamula et al. studied the heat transfer enhancement by a combination of impingement and cross flow-induced swirl in a two-pass channel<sup>39</sup>. Results show that the new impingement system, from the first pass to the second pass, using cross flow injection holes produce significantly higher heat transfer on the second pass walls.

### *Combined Effect of Swirl Flow and Ribs*

Kieda et al. experimentally investigated the single-phase water flow and heat transfer in a rectangular cross-sectioned twisted channel<sup>40</sup>. Several aspect ratios and twist pitches were used. Results indicate that in a cooling application, this twisted channel performs similar to a ribbed pipe. Zhang et al. used different types of inserts to study the combined rib and twisted tape inserts in square ducts<sup>41</sup>. Four test configurations were used: twisted tape, twisted tape with interrupted ribs, hemi-circular wavy tape, and hemi-triangular wavy tape. The twisted tape with interrupted ribs provides higher overall heat transfer performance over the twisted tape without ribs and

hemi-circular wavy tape. The performance of the hemi-triangular wavy tape is comparable with the twisted tape plus interrupted ribs. Hemi-circular wavy tapes show the lowest heat transfer performance in this group.

*Combined Effect of a Ribbed Wall with Grooves or Pins*

Zhang et al. studied the heat transfer and friction in rectangular channels with a rib-groove combination<sup>42</sup>. The Stanton numbers for the ribbed-grooved walls are higher than that for the only ribbed walls at similar rib spacing values. Metzger et al. indicated that the addition of ribs does not change the heat transfer coefficient from the pin-mounted surface<sup>43</sup>. However, the heat transfer coefficient on the rib surface is significantly higher than the pin-mounted surface.

*New Cooling Concepts*

Heat pipes have very high effective thermal performance<sup>44</sup>. Therefore, they can transfer heat from high temperature to the low temperature regions. This concept may be used in the airfoil cooling. Heat is removed from the initial stage stator airfoils and the heat is delivered at a later stage to heat up the main flow. This way the heat extracted can be recycled to the main flow. In a concept developed by Yamawaki et al., the heat is conducted away from the hot airfoil to the fin assembly<sup>45</sup>. This passive heat extraction reduces the required cooling air. Most heat pipe applications are designed for the stator airfoils, where it is easier to mount the connecting pipes or fins. Recently, Kerrebrock and Stickler proposed a design to incorporate heat pipe in the rotor<sup>46</sup>.

The concept of cooled cooling air systems, through a heat exchanger, for turbine thermal management was reported by Bruening and Chang<sup>47</sup>. Results show that the use of a cooled cooling air system can make a positive impact on overall engine performance for land-based turbines. Commonly a closed loop steam cooled nozzle with thermal barrier coatings (TBC) is used in order to reduce the hot gas temperature drop through the first stage nozzle (Corman and Paul<sup>48</sup>. A closed looped with mist/steam cooling was reported by Guo et al.<sup>49</sup>. Results show that an average heat transfer enhancement of 100% can be achieved with 5% mist (fine water droplets) compared to the steam cooling; similar results were reported by Li et al.<sup>50</sup>.

**4.2.2.2-3 Enhanced Internal Cooling of Turbine Blades**

Figure 6 shows several techniques to cool a modern gas turbine blade. The blade consists of serpentine cooling passages lined with rib turbulators. Jet impingement is used to cool the leading edge of the blade, and pin-fin cooling with ejection is used near the trailing edge. Although the techniques used to cool the blades are similar to those used to cool the vanes, the heat transfer trends in the vanes and blades are very different. Because the blades are rotating, the flow of the coolant in the passages is altered. Therefore, the effect of rotation on the internal heat transfer enhancement must be considered.

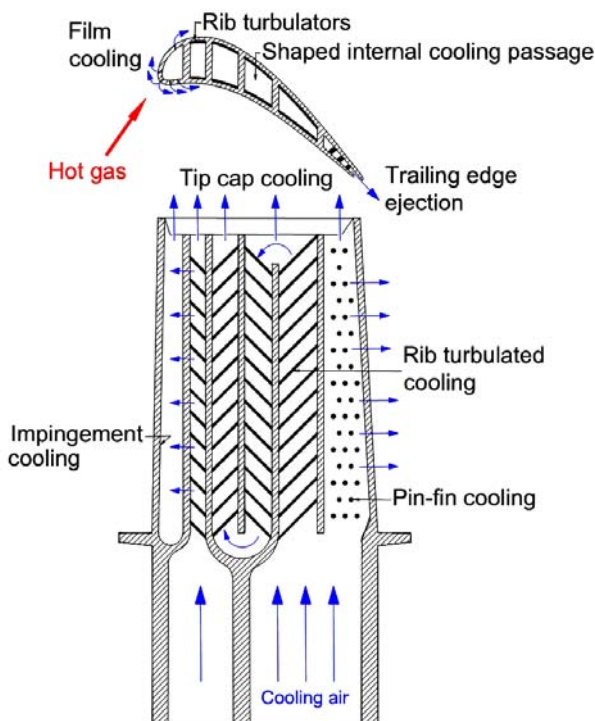


Fig. 6. Schematic of a Modern Gas Turbine Blade with Common Cooling Techniques

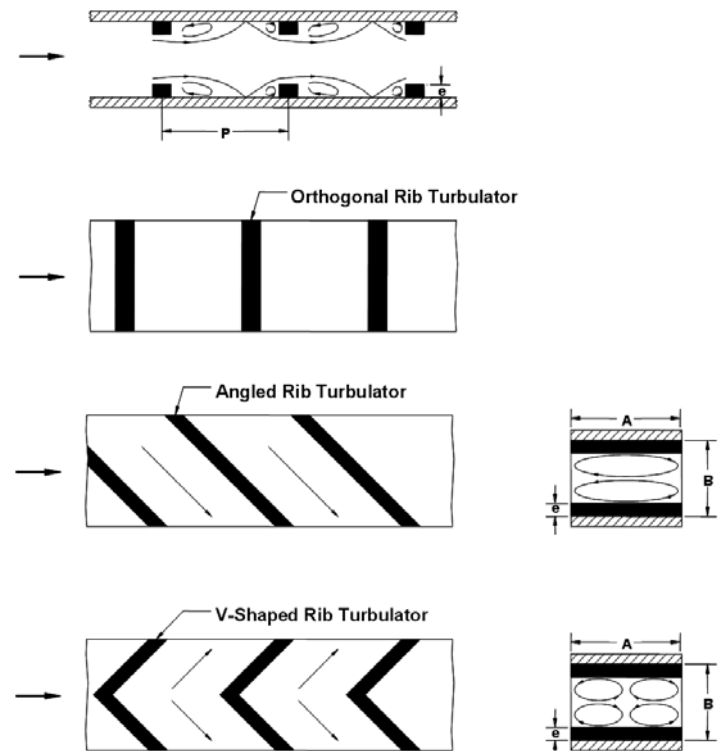


Fig. 7. A Typical Test Model for Turbulated Cooling Studies with Rib Induced Secondary Flow

### Rib Turbulated Cooling

Rib turbulators are the most frequently used method to enhance the heat transfer in the internal serpentine cooling passages. The rib turbulence promoters are typically cast on two opposite walls of the cooling passage. Heat that conducts from the pressure and suction surfaces through the blade walls is transferred to the coolant passing internally through the blade. The heat transfer performance of the ribbed channel depends on the channel aspect ratio, the rib configurations, and the Reynolds number of the coolant flow. Many fundamental studies have been conducted to understand the coolant flow through a stationary ribbed channel<sup>51</sup>. The studies show as the coolant passes over a rib oriented 90° to the mainstream flow, the flow near the channel wall separates. Reattachment follows the separation, and the boundary layer reattaches to the channel wall; this thinner, reattached boundary layer results in increased heat transfer coefficients in the ribbed channel. This rib induced secondary flow is shown in figure 7. If the rib turbulators are skewed to the mainstream flow direction, counter-rotating vortices are created. Figure 7 shows in a channel with angled ribs, two counter-rotating vortices are formed in the cross-section of the cooling passage. However, if V-shaped rib turbulators are used, four vortices are generated. The additional set of counter-rotating vortices associated with the V-shaped ribs results in more heat transfer enhancement in a channel with V-shaped ribs than angled ribs. The ribs also create turbulent mixing in the areas of flow separation. With this additional mixing, the heat is more effectively dissipated from the wall, and thus additional heat transfer enhancement. Because only the flow near the wall of the cooling channel is disturbed by the ribs, the pressure drop penalty by ribs affordable.

Han and Han and Park developed correlations for both the pressure penalty and heat transfer enhancement in ribbed channels<sup>52</sup>. Given the Reynolds number of the coolant flow and the rib geometry ( $e/D$ ,  $P/e$ ,  $W/H$ , and  $\alpha$ ), the average friction factor in a channel with two opposite ribbed walls,  $\bar{f}$ , and the centerline average Stanton number on the ribbed walls,  $St_p$ , can be determined from the correlations. Figure 8 demonstrates the correlations developed for cooling passages with 90° ribs. The friction roughness function,  $R$ , is only a function of rib spacing for the range of the roughness Reynolds number,  $e^+$ , shown. Based on the rib spacing ( $P/e$ ),  $R$  can be calculated, and substituted into the following equation to determine  $f$ , the four ribbed wall friction factor.

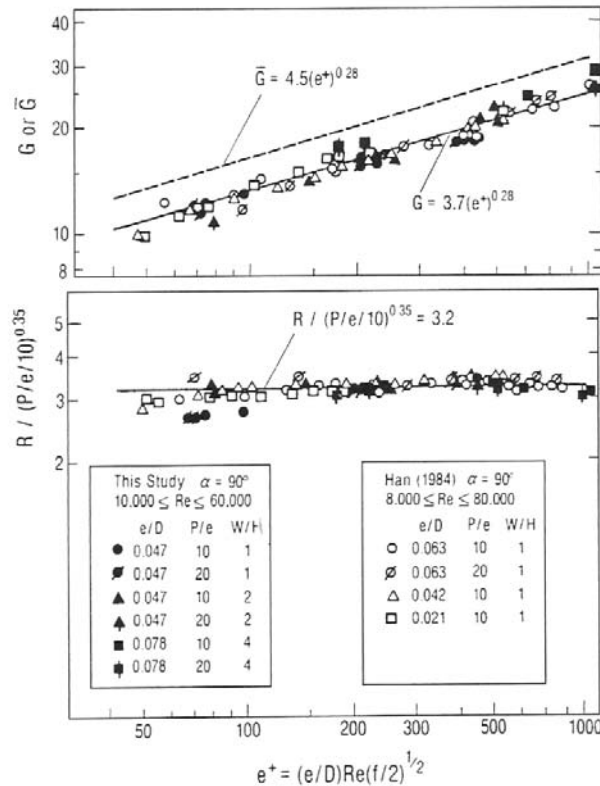


Fig. 8. Friction Factor and Heat Transfer Coefficient Correlations for 90° Ribs

$$R = \left(\frac{2}{f}\right)^{1/2} + 2.5 \ln \left(\frac{2e}{D} \cdot \frac{2W}{H+W}\right) + 2.5 \quad (1)$$

From  $f$  (the friction factor in a channel with ribs on all four walls) and the channel geometry ( $H/W$ ), the average friction factor in a channel with ribs on two walls,  $\bar{f}$ , can be calculated using Eqn. 2.



$$f = \bar{f} + \left(\frac{H}{W}\right)(\bar{f} - f_s) \tag{2}$$

The friction factor in a channel with smooth walls,  $f_s$ , is known from the existing Blasius correlation for smooth channel flow.

Using the four ribbed wall friction factor,  $f$ , the rib height,  $e/D$ , and the Reynolds number of the coolant flow,  $Re$ , the roughness Reynolds number,  $e^+$ , can be calculated using the definition shown in figure 8. From  $e^+$  the top figure can be used to obtain  $G$ , the heat transfer roughness function, and Eqn. 3 can be used to calculate the Stanton number on the ribbed walls,  $St_r$ .

$$G = R + \frac{\left(\frac{f}{2St_r}\right) - 1}{\left(\frac{f}{2}\right)^{1/2}} \tag{3}$$

The correlation shown in figure 8 is for a Prandtl number of 0.703. Because  $G$  is inversely proportional to the Stanton number, a low heat transfer roughness function implies high heat transfer from the cooling passage wall.

With the understanding that skewed ribs yield higher heat transfer enhancement than orthogonal ribs, these correlations were extended to include the effect of the rib angle. Figure 9 shows the correlations taking into account the rib angle,  $\alpha$ . From the rib angle ( $\alpha$ ), rib spacing ( $P/e$ ), and channel aspect ratio ( $W/H$ ), the roughness function,  $R$ , can be determined. Eqn. 1 can be used to calculate  $f$ , and Eqn. 2 is used to determine the friction factor in a channel with two ribbed walls. Similar to channels with  $90^\circ$  ribs,  $R$  and  $e^+$  are then used to determine the Stanton number on the ribbed walls. These correlations can be used over a wide range of channel aspect ratios and rib configurations; however one should refer to the original papers for specific restrictions of the correlations.

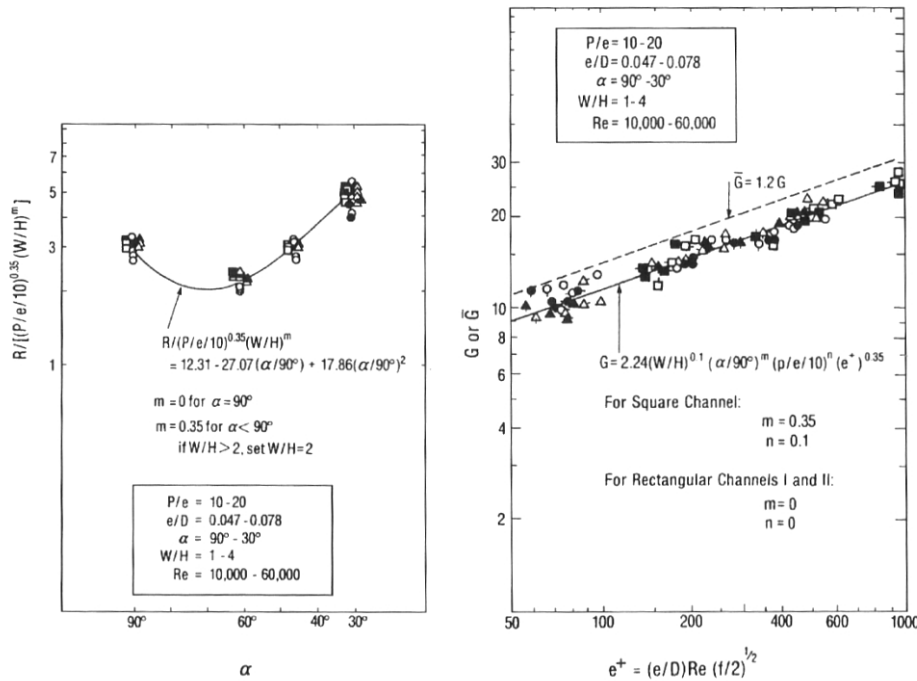


Fig. 9. Friction Factor and Heat Transfer Correlations in Rectangular Ribbed Channels

Because ribs are the most common heat transfer enhancement technique for the serpentine cooling passages, many studies have been conducted to study the effects of channel cross-section, rib configuration, and coolant flow Reynolds number. As shown in figure 6, the aspect ratio of the channels changes from the leading to the trailing edge of the blade. Near the leading edge of the blade, the channel may have an aspect ratio around  $1/4$ , but near the trailing edge, much broader channels are present with aspect ratios around 4.

Multiple studies have shown that by skewing the ribs, so they are angled into the mainstream flow, the heat transfer coefficients can be further enhanced. Placing the ribs with an attack angle between  $30^\circ$  and  $60^\circ$  results in increased heat transfer and reduces the pressure penalty. Most studies focus on Reynolds numbers ranging from 10,000 to 80,000, but for today's advanced gas turbines the coolant in the channel can have a Reynolds number up to 500,000. The height of the ribs is typically 5-10% of the channel hydraulic diameter, and the rib spacing-to-height ratio varies from 5 to 15. In addition, a limited number of studies have focused on the more closely spaced ribs with much larger blockage ratios.

## 4.2.2.2 Enhanced Internal Cooling of Turbine Blades and Vanes

With angled ribs performing superior to orthogonal ribs, many researchers have extended their studies to include a wide variety of rib configurations. Han et al. showed that V-shaped ribs (figure 10) outperform the angled ribs; for a given pressure drop, the V-shaped ribs give more heat transfer enhancement<sup>53</sup>. Numerous other studies have shown the same conclusion that V-shaped ribs perform better than the traditional angled ribs in a variety of channels and flow conditions<sup>54</sup>. In an effort to further increase the heat transfer performance of the rib turbulators, discrete rib configurations were introduced. Figure 10 shows discrete (or broken) ribs are similar to the traditional ribs, but they are broken in one or more locations, so the rib is not continuous. In the majority of cooling channels, discrete ribs were shown to outperform the continuous angled or V-shaped ribs and Cho et al.<sup>55</sup>. Han and Zhang compared the performance of many high performance rib configurations, and the comparison is shown in figure 11<sup>56</sup>. As shown in this figure, the broken 45° angled ribs create more heat transfer enhancement than the continuous 45° angled ribs at a given friction factor ratio, and this conclusion can be extended to other broken versus continuous rib configurations.

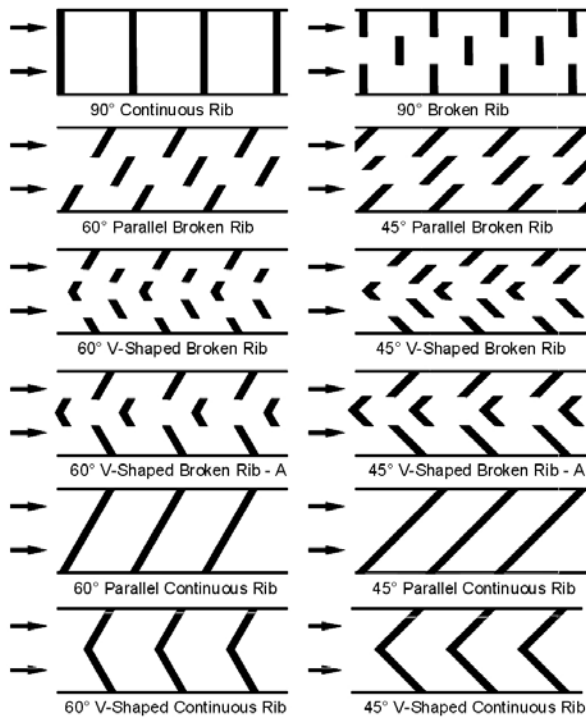


Fig. 10. High Performance Rib Turbulators for Turbine Blade Internal Cooling

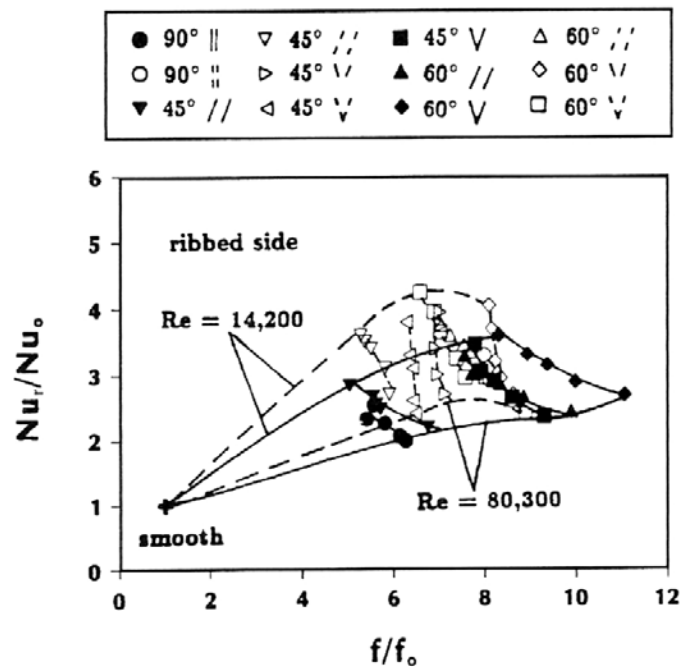


Fig. 11. Comparison of Heat Transfer Performance for Broken and Non-Broken Rib Configurations

The majority of ribs used in experimental studies have a square cross-section; however, studies have investigated the heat transfer enhancement of various profiled ribs. Delta-shaped ribs were studied by Han et al. and these ribs were also shown to result in higher heat transfer enhancement than the traditional angled ribs<sup>57</sup>. Bunker and Osgood investigated the performance of ribs leaning into or away from the flow<sup>58</sup>. They concluded the traditional square ribs give greater heat transfer enhancement and less frictional losses than the ribs leaning into or away from the flow.

When the blades are cast, the ribs are unlikely to have sharp edges as the previous studies have considered. The ribs are likely to have rounded edges, and this was taken into account by Taslim and Spring<sup>59</sup>. From their experimental work, they concluded the effect of rounding decreases the level of heat transfer enhancement in the cooling channel. Ribs with a higher aspect ratio (taller ribs) are more sensitive to the rounding effect; whereas, square ribs are only slightly affected by the rounded edges. However, the pressure drop is significantly less in the channels with rounded ribs.

Studies have also focused on ribbed channels with more blockage. Bailey and Bunker and Taslim and Spring showed that increasing in the effective blockage, the heat transfer coefficients can increase<sup>60</sup>. However, this increase comes at the cost of a significant increase in the pressure penalty. Therefore, if the heat loads are extremely high and the high frictional losses can be tolerated, the additional heat transfer enhancement would be beneficial.

An additional factor that should be considered when determining the heat transfer distribution in cooling channels is the decreasing coolant flow rate due to extraction for film cooling. Most modern turbine airfoils have ribs in the internal coolant channel and film cooling for the outside surface. Therefore, some of the cooling air is bled through the film cooling holes. The presence of periodic ribs and bleed holes creates strong axial and spanwise variations in the heat transfer distributions on the passage surface. Shen et al., Ekkad et al., and Thurman and Poinsette each studied the heat transfer enhancement by ribs in the presence of coolant extraction<sup>61</sup>. These studies showed that the heat transfer coefficients in the near-hole regions increase, but no broader impact by these holes is noticeable in these results. Ekkad et al. showed that the regional-averaged Nusselt number ratios for different rib orientations are almost identical with and without bleed hole extraction, as shown in figure 12<sup>62</sup>. This indicates that 20 to 25% reduction of the main flow can be used for film cooling without significantly affecting the ribbed channel cooling performance. It was also shown that the heat transfer near the holes can be further enhanced if the ribs are placed near the bleed holes<sup>63</sup>.

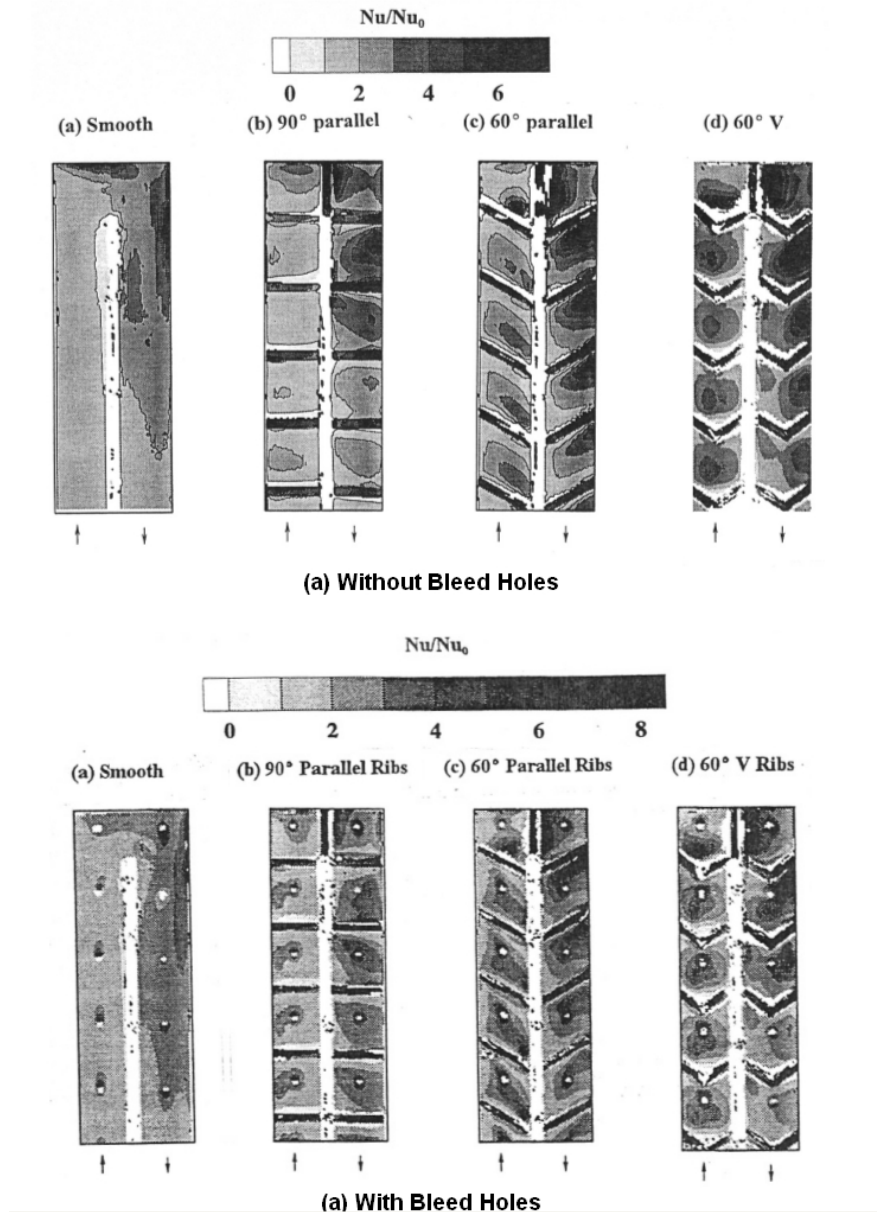


Fig. 12. Heat Transfer Enhancement in Cooling Passages with and without Film Coolant Extraction Holes

### *Rotational Effect on Rib Turbulated Cooling*

Heat transfer in rotating coolant passages is very different from that in stationary coolant passages. Both Coriolis and rotating buoyancy forces alter the flow and temperature profiles in the rotor coolant passages and affect their surface heat transfer coefficient distributions<sup>64</sup>. It is very important to determine the local heat transfer distributions in the rotor coolant passages under typical engine cooling flow, coolant-to-blade temperature difference (buoyancy effect), and rotating conditions. Effects of coolant passage cross-section and orientation on rotating heat transfer are also important. As sketched in figure 13, the secondary flows in a two-pass channel are different for radial outflow and radial inflow passes<sup>65</sup>. Since the direction of the Coriolis force is dependent on the direction of rotation and flow, the Coriolis force acts in different directions in the two-passes. For radial outward flow, the Coriolis force shifts the core flow towards the trailing wall. If both the trailing and leading walls are symmetrically heated, then the faster moving coolant near the trailing wall would be cooler (therefore heat transfer would be enhanced) than the slower moving coolant near the leading wall (i.e., heat transfer would be decreased). Rotational buoyancy is caused by a strong centrifugal force that pushes cooler heavier fluid away from the center of rotation. In the first channel rotational buoyancy affects the flow in a similar fashion as the Coriolis force and causes a further increase in flow and heat transfer near the trailing wall of the first channel; whereas, the Coriolis force favors the leading side of the second channel. The rotational buoyancy in the second channel tries to make the flow distribution more uniform in the duct.

## 4.2.2.2 Enhanced Internal Cooling of Turbine Blades and Vanes

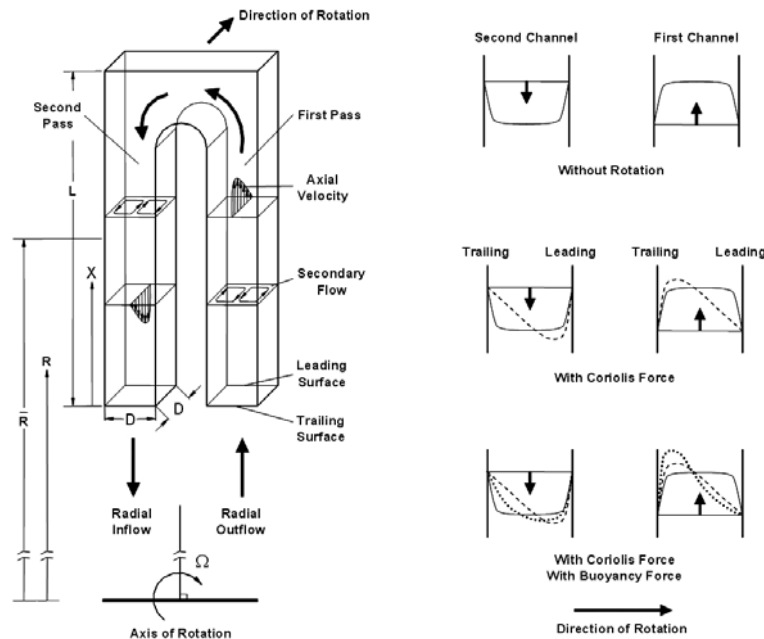


Fig. 13. Conceptual View of Coolant Flow through a Two-Pass Rotating Channel

### *Wall Heating Condition Effect on Rotating Coolant Passage Heat Transfer*

From the above analyses, the rotation effect on channel heat transfer comes from the Coriolis and centrifugal forces. The centrifugal force is known as rotation buoyancy when there is a temperature difference between the coolant and the channel walls under rotating conditions. Since the temperature difference between the coolant and the channel walls varies along the coolant passages, so does the rotation buoyancy. Therefore, it is expected that the channel wall heating conditions would affect rotor coolant passage heat transfer. The channel heating conditions imply that the channel walls may be at the same temperature (or heat flux) in both streamwise and circumferential directions, or the trailing wall temperature may be higher than the leading wall temperature in real turbine blade cooling applications. Han et al. studied the uneven wall temperature effect on rotating two-pass square channels with smooth walls<sup>66</sup>. They concluded that in the first pass, the local uneven wall temperature interacts with the Coriolis force-driven secondary flow and enhances the heat transfer coefficients in both leading and trailing surfaces, with a noticeable increase in the leading side, as compared with the uniform wall temperature case. However, the uneven wall temperature significantly enhances heat transfer coefficients on both leading and trailing surfaces. Parsons et al. and Zhang et al. studied the influence of wall heating condition on the local heat transfer coefficient in rotating two-pass square channels with 90° ribs and 60° ribs on the leading and trailing walls, respectively<sup>67</sup>. They concluded that the uneven wall temperature significantly enhances heat transfer coefficients on the first-pass leading and second-pass trailing surfaces as compared with the uniform wall temperature condition.

### *Combined Effect of Rotation and Rib Shape on the Heat Transfer in Rotating Channels*

The above studies investigating the effect of rotation on the heat transfer in cooling channels only consider the heat transfer in channels with square ribs. However, the shape of the rib can significantly alter the heat transfer trends, as demonstrated in stationary channels. Acharya et al. investigated the heat/mass transfer in a square, two-pass rotating channel with various profiled ribs placed on the leading and trailing surfaces<sup>68</sup>. It was shown that certain profiled ribs provide better heat transfer enhancement than the conventional square ribs. The smooth sidewalls of the channel also see significantly more enhancement than the smooth walls of channels with square ribs.

### *Effect of Channel Cross-Section and Channel Orientation on Rotating Channel Heat Transfer*

The first studies of heat transfer in rotating channels were performed on square channels oriented normal to the direction of rotation. Wagner et al. reported that the heat transfer coefficients on the trailing surface of the first pass can be enhanced 2-3 times that of a non-rotating channel, while the leading surface experiences a decline of up to 50%<sup>69</sup>. Opposite trends were present in the second pass of this smooth channel. The cooling channel was lined with angled turbulators, and it was found there is less of an effect of rotation in a ribbed channel than a smooth channel<sup>70</sup>. Because the heat transfer enhancement of the ribbed channel is already 3.5 times greater than that of a smooth channel, rotation does not provide the same percentage of enhancement in the cooling channel with ribs. However, the additional enhancement is significant and should be considered. Similar to the non-rotating channel, 45° angled ribs provide more enhancement than 90° ribs in a rotating channel. Park et al. conducted naphthalene sublimation experiments to examine the effects of rotation on the local heat and mass transfer distribution in a two-pass ribbed square channel<sup>71</sup>. They also found that the overall heat and mass transfer in a rotating channel with ribbed surfaces was not affected by the Coriolis force as much as that in a rotating channel with smooth surfaces.

When considering rotating channels, the orientation of the channels must be considered. One can see in figure 14 that the orientation of the channel changes as on moves away from the middle of the blade. Johnson et al. studied the effects of rotation on the heat transfer for smooth and 45° ribbed serpentine channels with channel orientations of 0° and 45° to the axis of rotation<sup>72</sup>. They found that the effects of Coriolis and buoyancy forces on heat transfer in the rotating channel are decreased with the channel at 45° compared to the results at 0°. This implies that the difference in heat transfer coefficient between the leading and trailing surfaces due to rotation will be reduced when the channel is angled to the axis of rotation. Parsons et al. investigated the effect of channel orientation on the heat transfer in a rotating, square two-pass channel with 60° angled ribs<sup>73</sup>. They also concluded that difference between the heat transfer coefficients on the leading and trailing surfaces decreases when the orientation of the channel changes from 90° to 45°.

Dutta and Han conducted an experimental study of regionally averaged heat transfer coefficients in rotating smooth and ribbed two-pass channels; this study also investigated the effect of channel orientation on the heat transfer distributions in this square channel<sup>74</sup>. They found the effect of rotation is reduced for non-orthogonal alignment of the heat transfer surfaces with respect to the plane of rotation. They also concluded that the discrete V-shaped ribs have better heat transfer performance than the 90° ribs and the 60° angled ribs in the rotating channels. Al-Hadhrami and Han used parallel and crossed 45° angled ribs in rotating two-pass square channels to study the effect of channel orientation on heat transfer<sup>75</sup>. They concluded that the parallel 45° angled ribs are better than the crossed 45° angled ribs. They also confirmed the difference between the leading and trailing wall heat transfer coefficients is reduced for the channel with a 45° angle to the axis of rotation.

As shown in figure 14, the cross-section of the cooling channels can vary depending on where the cooling channel is located within the blade. Studies showed the heat transfer distributions in square channels can vary significantly from those in rectangular channels. Therefore, it is necessary to study the effect of rotation on heat transfer in rectangular channels. As with the square channels, the orientation of the channel varies depending on the location in the blade.

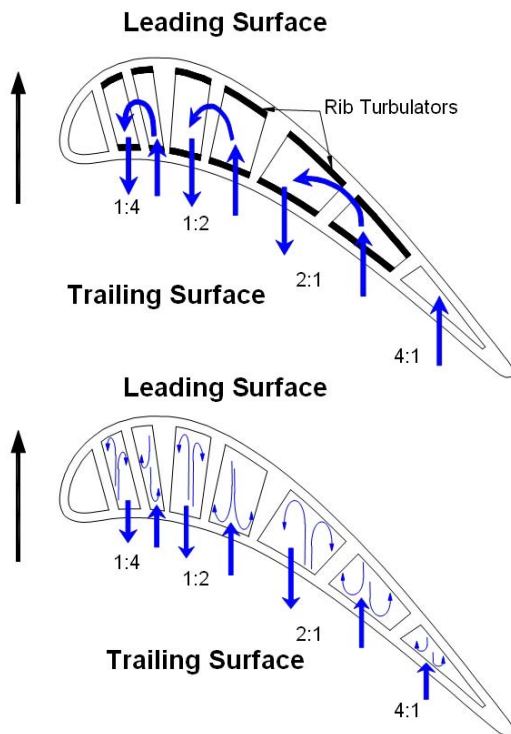


Fig. 14. Typical Cooling Passage Size and Orientation with Conceptual Views of the Rotation Induced Secondary Flow

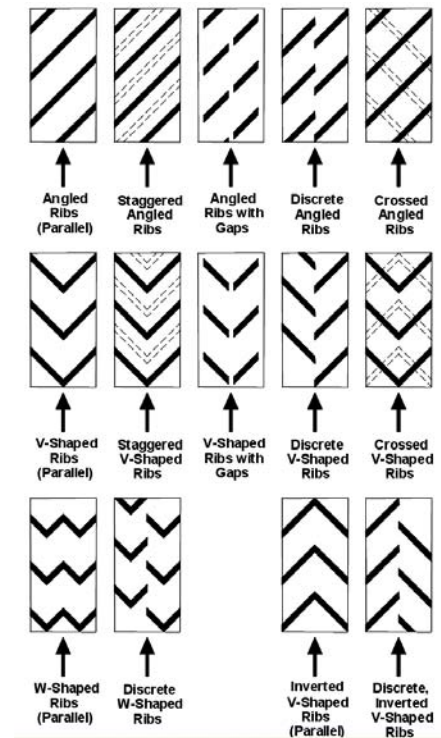


Fig. 15. Advanced Rib Configurations Studied in Rotating Cooling Channels

Guidez reported the effect of rotation on heat transfer in a straight rotating rectangular channel ( $AR = 2:1$ ) with smooth walls<sup>76</sup>. Soong et al. conducted heat transfer experiments in rotating smooth straight duct with different aspect ratios ranging from 0.2 to 5.0<sup>77</sup>. They concluded that the aspect ratio of the duct was a critical parameter in the secondary flow patterns. Taslim et al. investigated the varying effect of rotation in square ( $AR = 1:1$ ) and rectangular ( $AR = 2:1$ ) with 45° crossed ribs<sup>78</sup>. Azad et al. and Al-Hadhrami et al. studied heat transfer in a two-pass rectangular rotating channel ( $AR = 2:1$ ) with 45° angled ribs and 45° V-shaped ribs, respectively, including the effect of channel orientation with respect to the axis of rotation<sup>79</sup>. The heat transfer trends in these rectangular channels are similar to those of square channels: the heat transfer on trailing surface of the first pass is enhanced with rotation while the heat transfer on the leading surface decreases (and the opposite is true in the second pass). However, the difference between the leading and trailing surfaces decreases in the 2:1 rectangular channels. As the orientation of the channels varies from 90° to 45°, the effect of rotation continues to decrease. Similar to non-rotating channels, these studies concluded that the 45° V-shaped ribs perform better than the 45° crossed V-shaped ribs, and subsequently better than 45° angled ribs (figure 15).

## 4.2.2.2 Enhanced Internal Cooling of Turbine Blades and Vanes

Moving closer to the trailing edge, the aspect ratio of the cooling channels continues to increase, as the channel orientation is also changing. Griffith et al. studied heat transfer in a single pass rectangular channel (AR = 4:1) with smooth and 45° angled ribbed walls, including the effect of channel orientation with respect to the axis of rotation<sup>80</sup>. Results show that the narrow rectangular passage exhibits much higher heat transfer enhancement for the ribbed surface than the square and 2:1 channels previously investigated. Also, channel orientation significantly affects the leading and side surfaces, yet does not have much affect on the trailing surfaces for both smooth and ribbed surfaces. Therefore, this investigation has determined that spanwise variations in the heat transfer distribution of rectangular cooling passages exist, and that the enhancement is a function of channel orientation with respect to the axis of rotation, surface configuration (such as smooth or 45° angled ribbed walls), and channel aspect ratio. Lee et al. also studied the heat transfer in a single pass rectangular channel (AR = 4:1)<sup>81</sup>; they compared the heat transfer performance of V-shaped and angled rib turbulators with and without gaps (figure 15), in a channel oriented at 135° to the axis of rotation. The results show that V-shaped rib configuration produces more heat transfer enhancement than the angled rib configurations for both the stationary and rotating cases. There is only negligible difference in heat transfer enhancement between the parallel and staggered rib configurations for both the stationary and rotating cases. The results also show that the V-shaped ribs with gaps produce overall less heat transfer enhancement than the V-shaped ribs without gaps; whereas the angled ribs with gaps produce overall greater heat transfer enhancement than the angled ribs without gaps for the stationary case, and clearly the same enhancement for the rotating case. Most importantly, for narrow rectangular rib-turbulated channels oriented at 135° with respect to the plane of rotation, heat transfer enhancement on both the leading and trailing surfaces increases with rotation. This is quite different from the square channel where rotation enhances the trailing surface heat transfer but reduces the leading surface heat transfer for the radial outward flow case. This provides positive information for the cooling designers. Wright et al. expanded the study of the 4:1 channel with ribs to examine not only the heat transfer performance, but the overall thermal performance<sup>82</sup>. They investigated channels with six rib configurations: angled, V-shaped, W-shaped, discrete angled, discrete V-shaped, and discrete W-shaped (figure 15). Figure 16 shows that similar to the stationary channels, the rotating channel with discrete V-shaped ribs produced more heat transfer than the V-shaped and angled ribbed channels. However, the W-shaped and discrete W-shaped ribs yielded more heat transfer enhancement than the discrete V-shaped ribs. However, the increased heat transfer enhancement in the W-shaped and discrete W-shaped ribs came at the cost of an increased pressure penalty; these two configurations resulted in greatest pressure drop of the six configurations considered. Therefore, the overall performance of the discrete V-shaped and W-shaped ribs is comparable in the rotating channels. The traditional angled ribs exhibited the worst overall performance.

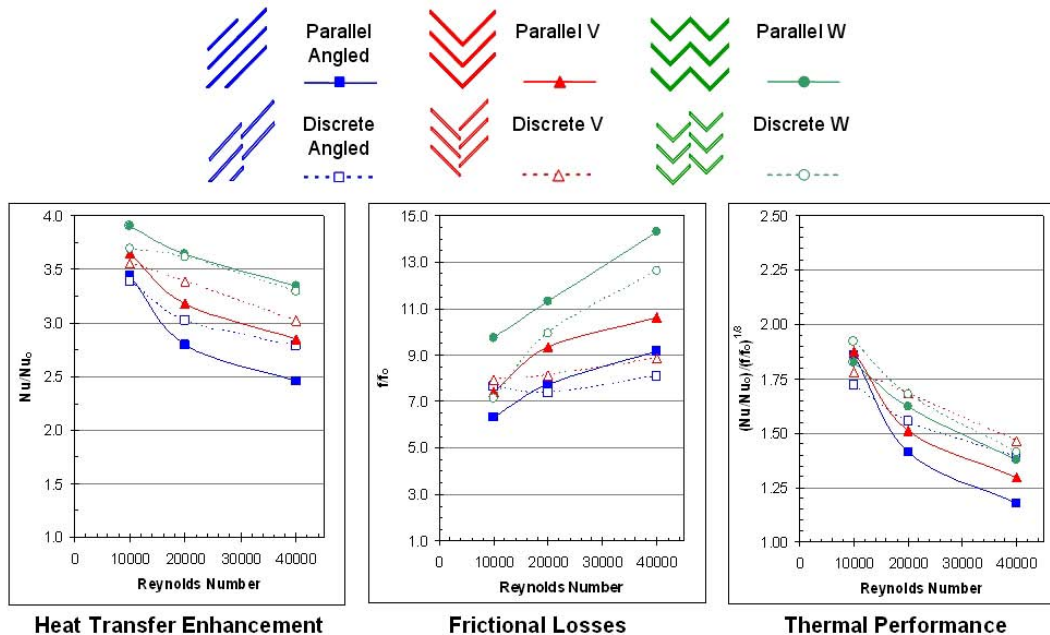


Fig. 16. Heat Transfer Enhancement, Frictional Losses, and Thermal Performance of Various Rib Configurations in a 4:1 Rotating Cooling Passage

The cooling channels near the leading edge of the blade typically a smaller aspect ratio compared to those near the center of the blade. Cho et al. studied the effect of rotation on heat transfer with a naphthalene sublimation technique in a two-pass rectangular channel (AR = 1:2) with smooth and 70° ribbed walls<sup>83</sup>. They found that the effect of rotation diminishes in the second pass with inward flow due to the strong influence of the 180° turn. This is quite different from the heat transfer trends found in the two-pass rectangular channels with aspect ratios greater than unity. Agarwal et al. reported the effect of rotation on heat transfer with naphthalene sublimation technique in two-pass rectangular channels (aspect ratio = 1:1 and 1:4) with smooth and 90° ribbed walls<sup>84</sup>. They concluded that the 1:4 rectangular channel provides lower levels of heat transfer enhancement along the trailing wall and higher levels of heat transfer degradation along the leading wall compared to the 1:1 square channel. Fu et al. also experimentally investigated the heat transfer trends

in cooling channels located near the leading edge of the blade<sup>85</sup>. The regionally averaged heat transfer coefficients in rotating cooling channels with aspect ratios of 1:4 and 1:2 lined with 45° angled ribs were obtained. This study concluded the rotation effect increased heat transfer on the trailing wall but decreased the heat transfer on the leading wall in the first pass of both the 1:4 and 1:2 channels. In the second pass, the difference of the heat transfer between the leading and trailing walls was reduced under the rotating condition when compared to the first pass. This study included the effect of channel orientation, and it was shown that the 45° channel orientation creates less heat transfer difference between the leading and trailing walls than the 90° channel orientation for both aspect ratio ducts. Rotation has a relatively small effect in the second pass of the 1:2 and 1:4 channels. It was suggested that the 180° turn induced vortices dominate the rotation induced vortices for the low aspect ratio ducts. When the results from this study were compared to others with various aspect ratios, it could be seen that the leading wall heat transfer has a strong dependence on the buoyancy parameter for 1:2 and 1:4 ducts in the first pass with radial outward flow, but it has a weak dependence on the buoyancy parameter for 2:1 and 4:1 ducts. Increasing the buoyancy parameter reduced the heat transfer on the leading walls for the 1:2 and 1:4 ducts in the first pass. The 1:4 duct has the largest heat transfer difference between the leading and trailing walls in the first pass.

Although the majority of rotating studies have focused on the heat transfer in square or rectangular cooling channels, a limited number of studies have focused on the heat transfer in channels with other cross-sections. Channels with a triangular cross-section might be used on some portion of the blade in order to provide compact channel structure and good cooling efficiency. Clifford et al. studied the mean heat transfer in a straight triangular-sectioned rotating duct with smooth walls<sup>86</sup>. Harasgama and Morris compared the effect of rotation on heat transfer in straight circular, triangular, and square duct with smooth walls<sup>87</sup>. Dutta et al. studied the effect of rotation on the heat transfer coefficients in two-pass triangular channels with smooth and ribbed walls<sup>88</sup>. For the locations in the first pass, the triangular-duct heat transfer coefficients are mostly contained within the upper and lower limits imposed by the square duct. This is because in a triangular duct, there is less space for the coolant to form secondary flow by rotation. However, in the second pass, the leading surface of the triangular duct shows much higher heat transfer coefficients than the square duct. This is due to more mixing and favorable secondary flow in the 180° turn for the triangular duct geometry. Rathjen et al. investigated the heat/mass transfer in a two-pass rotating channel with a near-engine cross-section; the first pass of the channel (radial outward) was trapezoidal, and the second pass (radial inward) had a larger trapezoidal cross-section<sup>89</sup>. They showed strong gradients after the 180° turn as the flow is forced to follow the shape of the blade.

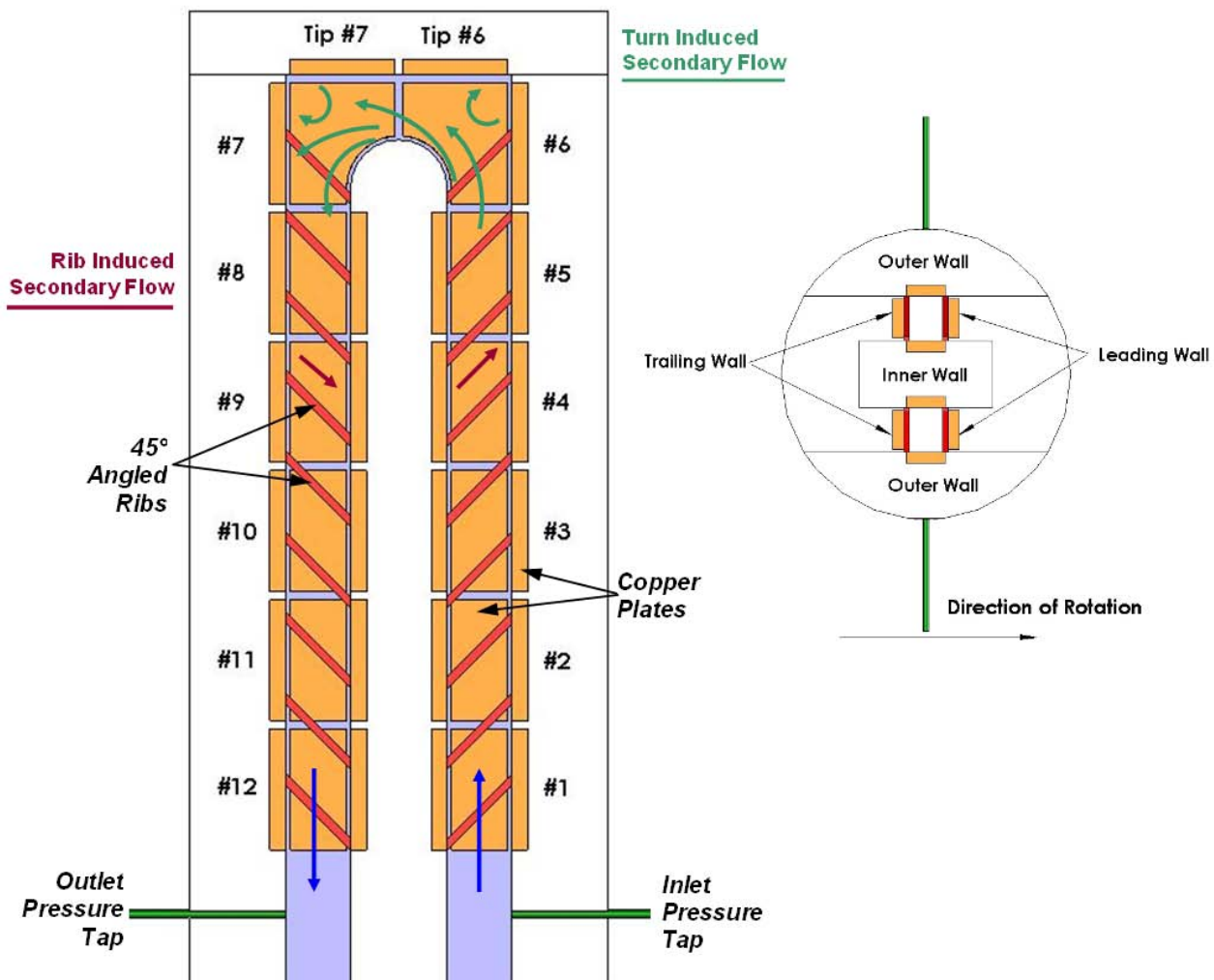


Fig. 17. Typical Experimental, Two-Pass Test Section with 45° Angled Ribs with a Conceptual View of the Rib and Turn Induced Secondary Flow

## 4.2.2.2 Enhanced Internal Cooling of Turbine Blades and Vanes

With the internal cooling passages of the blade can take on a variety of shapes, sizes, and orientations, it is interesting to investigate the effect of rotation in more detail. Results drawn from Fu et al. are presented to show the isolated affect of rotation on the heat transfer enhancement in channels with aspect ratios ranging from 1:4 (near the leading edge) to 4:1 (in the trailing edge region)<sup>90</sup>. Specifically, they studied two-pass channels with aspect ratios of 1:4, 1:2, 1:1, and 2:1, and they included the work of Griffith et al. to incorporate a 4:1 single pass cooling channel<sup>91</sup>. As shown by the sample test section in figure 17, each of the two-pass test sections consists of twelve regions in the stream-wise direction; with region one at the inlet of the test section, and region twelve at the outlet. Because the hydraulic diameter of each channel is different, comparisons are made at specific regions (1 through 12), rather than specific  $x/D$  locations, and the regions are labeled in figure 17. Figures 18-21 show the Nusselt number ratios at various regions in rotating channels with smooth walls, oriented at  $90^\circ$  to the direction of rotation, and figures 22-25 compare the heat transfer enhancement in cooling channels with smooth walls with various channel orientations (incorporating the probable channel location and orientation in an actual blade). This comparison is extended to rotating channels with  $45^\circ$  angled ribs in figures 26-33. The Nusselt number ratio shown is the measured Nusselt number in the rotating channel ( $Nu_R$ ) – – the Nusselt number measured in the identical stationary channel ( $Nu_S$ ). With this altered definition of the Nusselt number ratio, the effect of rotation is isolated from other factors influencing the heat transfer enhancement. In addition, the Nusselt number ratio is presented as a function of the local buoyancy parameter.

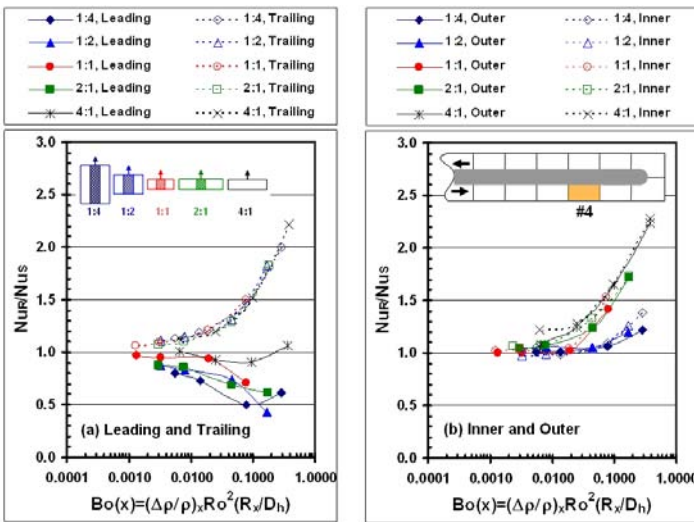


Fig. 18. Nusselt Number Ratio Comparison at Region 4 (1<sup>st</sup> Pass, Fully Developed) in Smooth Rotating Channels ( $\beta = 90^\circ$ )

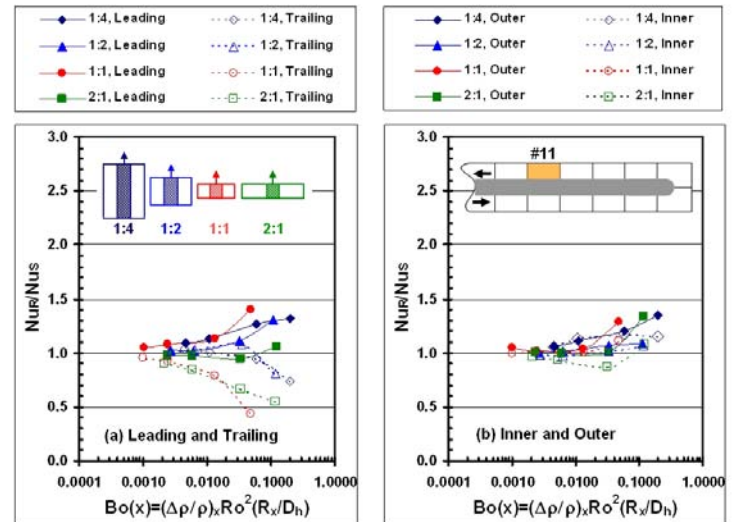


Fig. 19. Nusselt Number Ratio Comparison at Region 11 (2<sup>nd</sup> Pass, Fully Developed) in Smooth Rotating Channels ( $\beta = 90^\circ$ )

Figure 18 shows the Nusselt number ratios in region 4, on the leading and trailing surfaces (figure 18a), and the inner and outer surfaces (figure 18b); region 4 should represent fully developed flow in the first pass of each channel. The effect of rotation is most clearly seen on the trailing surface of the various channels. As the buoyancy parameter increases, the Nusselt number ratio increases in each channel, and the buoyancy parameter approaches zero, the Nusselt number approaches unity, as the effect of rotation diminishes. As explained earlier (and depicted in figure 13), the Coriolis and buoyancy forces combine to enhance the heat transfer coefficients on the trailing (destabilized) surface. Interestingly, the Nusselt number ratios on the trailing surfaces of the various channels all collapse to the same trend. The increase of the heat transfer coefficients on the trailing surface comes at the expense of the degradation of the heat transfer coefficients on the leading surface. In general, as the buoyancy parameter increases, the Nusselt number ratios decrease; indicating the adverse effect of rotation. However, the Nusselt number ratios cover a larger range than the ratios on the trailing surface. Positive information for turbine designers is shown in figure 18(b). As the buoyancy parameter increases, the Nusselt number ratios on both the inner and outer surfaces at region 4 increase.

Figure 19 moves to region 11 in the second pass; this region is far away from the  $180^\circ$  turn, so it should represent fully developed flow in the second pass. As shown in figure 19, the overall effect of rotation is reduced (when compared to the first pass) in second pass as the Coriolis and buoyancy forces act in opposite directions. Although the effect of rotation is expected to decrease, previous studies have shown, it is not eliminated, and this is further confirmed in figure 19. The leading surfaces of each channel experience heat transfer enhancement as the buoyancy parameter increases. However, the heat transfer enhancement due to rotation is much less on the leading surface of the second pass, than the trailing surface of the first pass. As shown in figure 18a, the enhancement due to rotation on the trailing surfaces increases the Nusselt number ratio up to (and beyond in the 4:1 channel) two times that of the stationary channel. However, on the leading surfaces in the second pass, the maximum heat transfer enhancement due to rotation does not exceed 1.5. As expected the trailing surfaces are adversely affected by rotation, with the 1:1 and 2:1 channels experiencing the greatest declination. The heat transfer coefficients on all of the inner and outer surfaces of region 11 are slightly enhanced with rotation, as shown in figure 19(b). However, the level of enhancement in this region is less than the enhancement in the first pass at region 4.



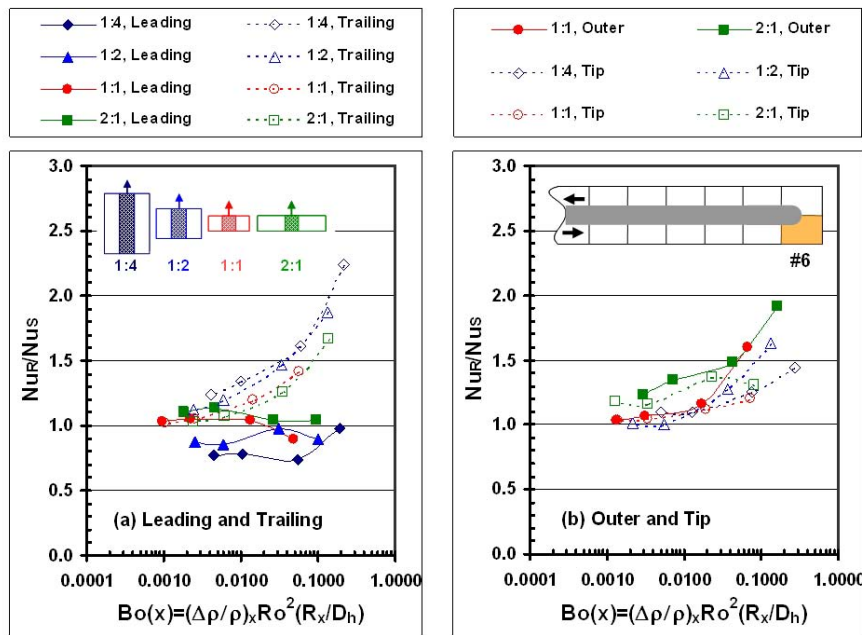


Fig. 20. Nusselt Number Ratio Comparison at Region 6 (1<sup>st</sup> Pass Turn) in Smooth Rotating Channels ( $\beta = 90^\circ$ )

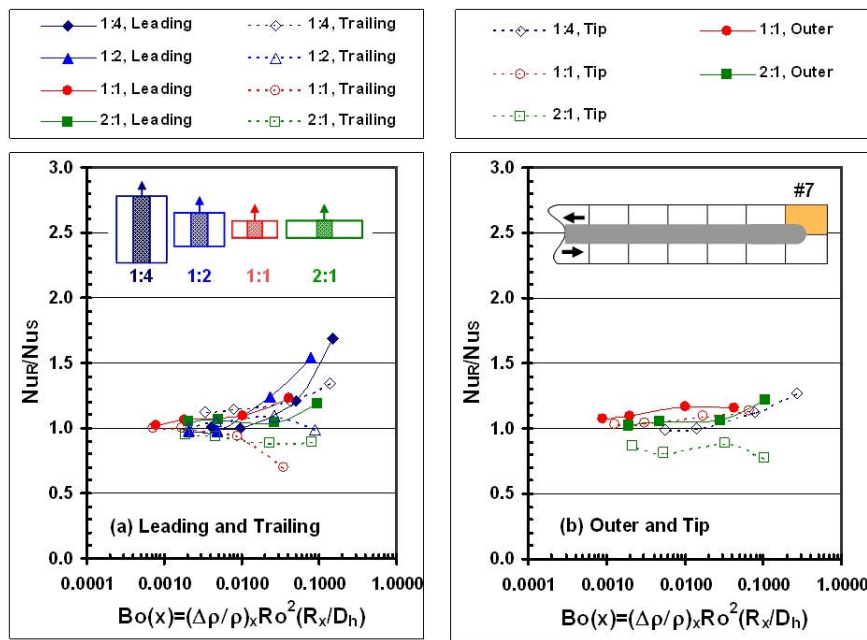


Fig. 21. A Nusselt Number Ratio Comparison at Region 7 (2<sup>nd</sup> Pass Turn) in Smooth Rotating Channels ( $\beta = 90^\circ$ )

In addition to considering the fully developed regions in the two-pass channel, the level of heat transfer enhancement in the sharp turn should also be considered. Figure 20 shows the Nusselt number ratios at region 6 for the leading, trailing, inner, and outer surfaces. Similar to region 4, the trailing surfaces at region 6 all experience heat transfer enhancement due to rotation. While the Nusselt number ratios for the leading surfaces are generally below unity. The variation between the leading and trailing surfaces is less than the difference in region 4, due to the onset of the sharp turn. As figure 20(b) shows, the heat transfer coefficients on both the outer and tip surfaces of region 6 are enhanced with rotation.

Figure 21 shows the Nusselt number ratios in region 7 (the second half of the sharp turn). The Nusselt number ratios on the leading surfaces in all the channels increase with the increasing buoyancy parameter, similar to region 11. With the exception of the 1:4 channel, the heat transfer coefficients on all of the trailing surfaces decreases with rotation. The effect of rotation on the outer and tip surfaces of region 7 is less than the effect of rotation in region 6. With the exception of the tip surface in the 2:1 channel, both the outer and tip surfaces are slightly elevated above the Nusselt number ratio of unity, and increasing the buoyancy parameter does not result in a significant increase in the Nusselt number ratios. With the flow redirection created in the stationary channel, the heat transfer coefficients are naturally elevated. Therefore, the additional secondary flow induced by rotation only slightly increases the already elevated Nusselt numbers.

## 4.2.2.2 Enhanced Internal Cooling of Turbine Blades and Vanes

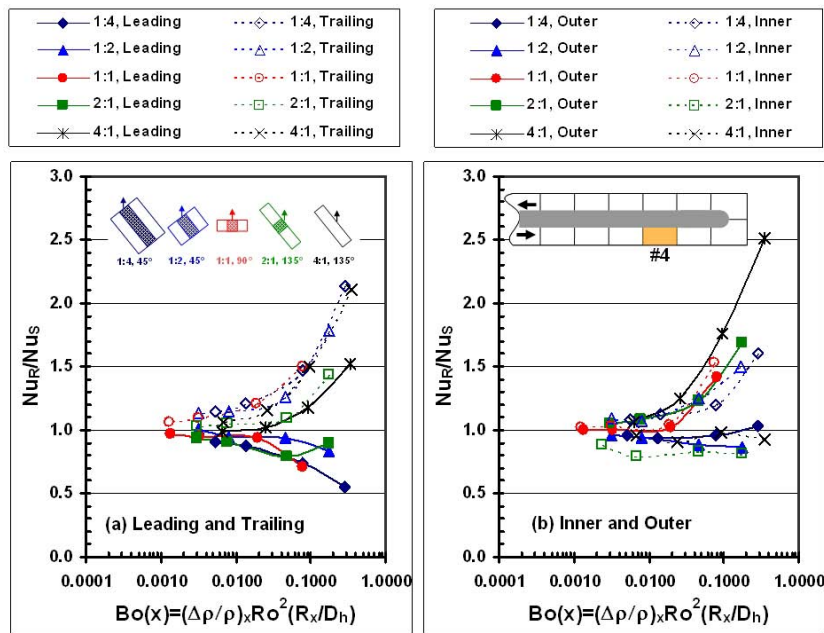


Fig. 22. Nusselt Number Ratio Comparison at Region 4 (1<sup>st</sup> Pass, Fully Developed) in Smooth Rotating Channels ( $\beta = 45^\circ$  or  $135^\circ$ )

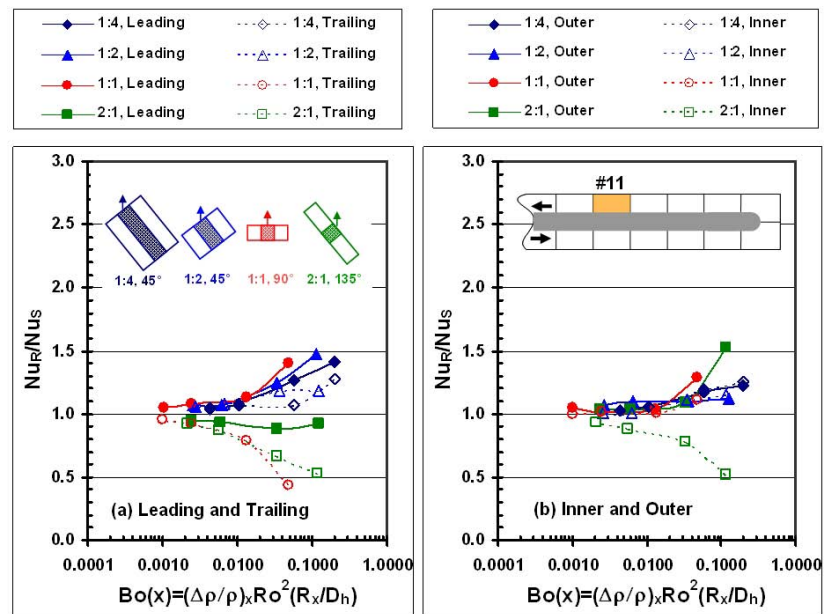


Fig. 23. Nusselt Number Ratio Comparison at Region 11 (2<sup>nd</sup> Pass, Fully Developed) in Smooth Rotating Channels ( $\beta = 45^\circ$  or  $135^\circ$ )

The effect of channel orientation is combined with the channel aspect ratio and local buoyancy parameters in figures 22 – 25. The 1:4 and 1:2 channels have orientations of  $45^\circ$ , the 2:1 and 4:1 channel are oriented at  $135^\circ$ , and the 1:1 channel maintains its previous orientation of  $90^\circ$ . As shown in figure 22, in the fully developed region of the first pass (region 4), the level of heat transfer enhancement on the trailing surfaces, due to rotation, is the same as in the channels with the  $90^\circ$  orientation. However, the degradation due to rotation on the leading surfaces is less in these skewed channels. Unlike the inner and outer surfaces of the channels with the  $90^\circ$  orientation, not all surfaces of every channel experience heat transfer enhancement with the increasing buoyancy parameter. The heat transfer enhancement (or decline) is strongly dependent on the channel aspect ratio. As shown in figure 14, the channel orientation affects the rotation induced vortices. In the 1:4 and 1:2 channels with the  $45^\circ$  channel orientation, the vortices are impinging on the inner surfaces of the first pass; thus increasing the heat transfer coefficients. However, the  $135^\circ$  of the 2:1 channel results in the vortices impinging on the outer surface, further increasing the heat transfer coefficients on the outer surface, rather than the inner surface.

The Nusselt number ratios at region 11 in the smooth channels with skewed orientations are shown in figure 23. The heat transfer enhancement on the leading surfaces of these skewed channels is similar to those with the normal orientation. However, the Nusselt numbers on the trailing surfaces of the 1:4 and 1:2 channels are increased with rotation; this differs from the orthogonal rotating

channels. The Nusselt numbers on the trailing surface 2:1 channel with the 135° orientation decrease with the increasing buoyancy parameter (similar the 2:1 channel with the 90° orientation). The level of heat transfer enhancement on the inner and outer walls in the second pass of these channels with various orientation is similar to the orthogonally rotating channels, with the exception of the inner wall of the 2:1 channel. The coolant is forced away from the corner between the inner and trailing walls to the corner between the leading and outer wall of the second pass. As the heat transfer coefficients on the trailing surface of the 2:1 channel sharply decrease, so do the heat transfer coefficients on the inner surface.

The additional complexity of flow through the sharp 180° turn is shown in figures 24 and 25. The level of heat transfer enhancement is the same on the leading and trailing surfaces, as well as the outer and tip surfaces of region 6. The dominant flow behavior through the turn is not strongly effected by the channel orientation; therefore, the Nusselt number ratios are not strongly effected as the channel orientation shifts from 90°, and these conclusions can be extended to region 7 of the channels, as well (figure 25).

The internal cooling passages of turbine blades generally do not have smooth surfaces. Therefore, it is important to consider not only channels with smooth walls, but cooling channels with rib turbulators. As described in previous sections, angled rib turbulators are commonly used in the blades. Fu et al. experimentally studied the effect of buoyancy on the heat transfer enhancement in channels with rib turbulators as they did for smooth, rotating passages. Figures 26 – 29 show rotating – to – stationary Nusselt number ratios at various regions in orthogonal cooling passages with angled ribs<sup>92</sup>.

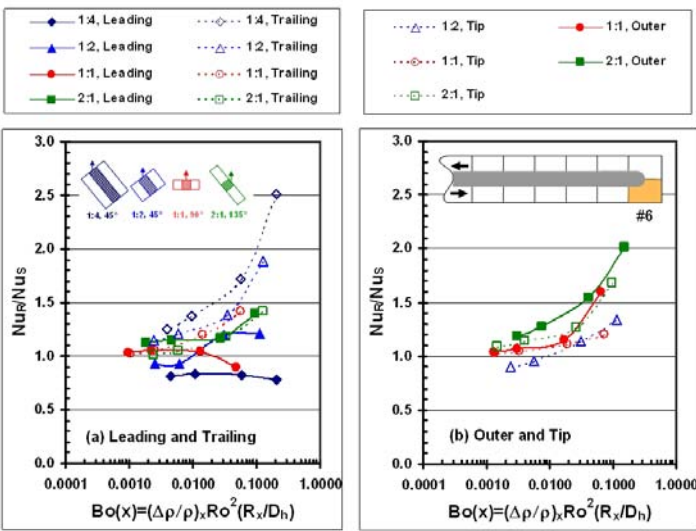


Fig. 24. Nusselt Number Ratio Comparison at Region 6 (1<sup>st</sup> Pass Turn) in Smooth Rotating Channels ( $\beta = 45^\circ$  or  $135^\circ$ )

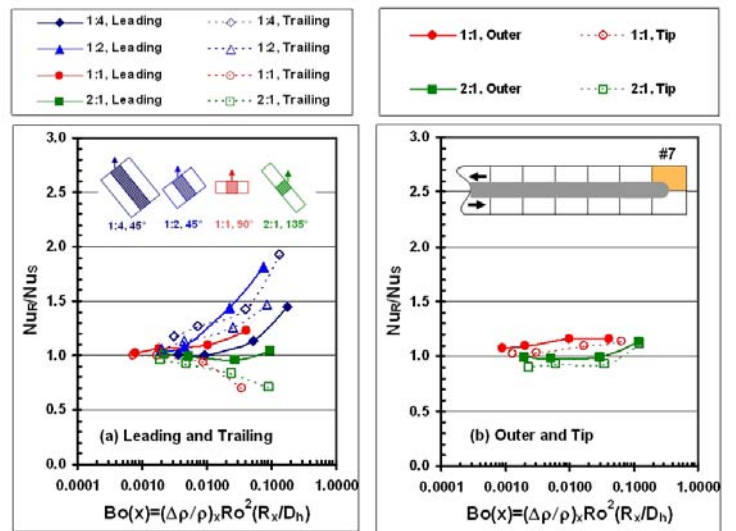


Fig. 25. Nusselt Number Ratio Comparison at Region 7 (2<sup>nd</sup> Pass Turn) in Smooth Rotating Channels ( $\beta = 45^\circ$  or  $135^\circ$ )

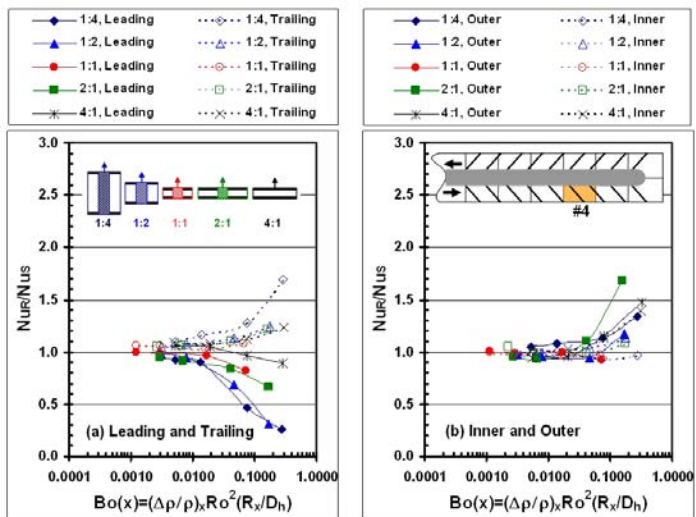


Fig. 26. Nusselt Number Ratio Comparison at Region 4 (1<sup>st</sup> Pass, Fully Developed) in Rotating Channels ( $\beta = 90^\circ$ ) with 45° Angled Ribs

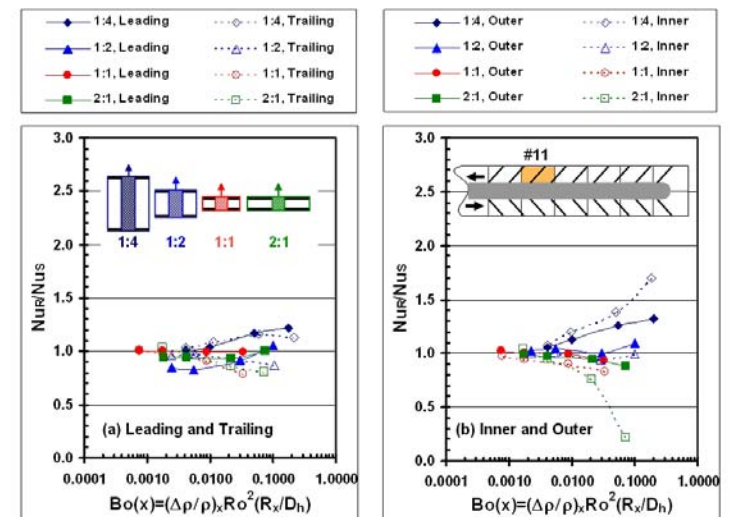


Fig. 27. Nusselt Number Ratio Comparison at Region 11 (2<sup>nd</sup> Pass, Fully Developed) in Rotating Channels ( $\beta = 90^\circ$ ) with 45° Angled Ribs

## 4.2.2.2 Enhanced Internal Cooling of Turbine Blades and Vanes

Figure 26 shows the effect of rotation on the heat transfer coefficients at region 4 in the cooling channels with 45° angled ribs. The general trends for the trailing (enhancement) and leading (declination) surfaces is same as for the smooth channel, as figure 26(a) shows. However, the effect of rotation on the trailing surface is less in the ribbed channels than the smooth channels. The Nusselt number ratios in the stationary channel are elevated to the presence of the ribs, and additional enhancement due to rotation is less significant in these ribbed channels. The declination of the heat transfer coefficients on the leading surface is more severe in these ribbed channels than the smooth channels; this is markedly clear in the 1:4 and 1:2 channels. From the numerical predictions of Su et al., the interaction of the rotation and rib induced secondary flow creates flow reversal, and a small cell of relatively hot air is trapped near the leading surface<sup>93</sup>. Within this cell, less mixing occurs with the core of the coolant flow, and therefore, these leading surfaces are adversely affected by rotation. Figure 26(b) shows that the Nusselt number ratios on both the inner and outer surfaces in region 4 are enhanced with rotation.

Figure 27 shows the effect of rotation is reduced in the second pass at region 11 when compared to the first pass at region 4. In addition the effect of rotation on the leading and trailing surfaces is less in these ribbed channels than the smooth channels. The heat transfer enhancement on the inner and outer surfaces at region 11 is strongly dependent on the channel cross-section. The 1:4 channel is most strongly affected by rotation; both the inner and outer surfaces experience heat transfer enhancement. The Nusselt number ratios of the remaining channels are not significantly affected by rotation, as the Nusselt number ratios are approximately unity over the range of buoyancy parameters. The inner surface of the 2:1 channels is the exception as a sharp decrease in the Nusselt number ratio is observed.

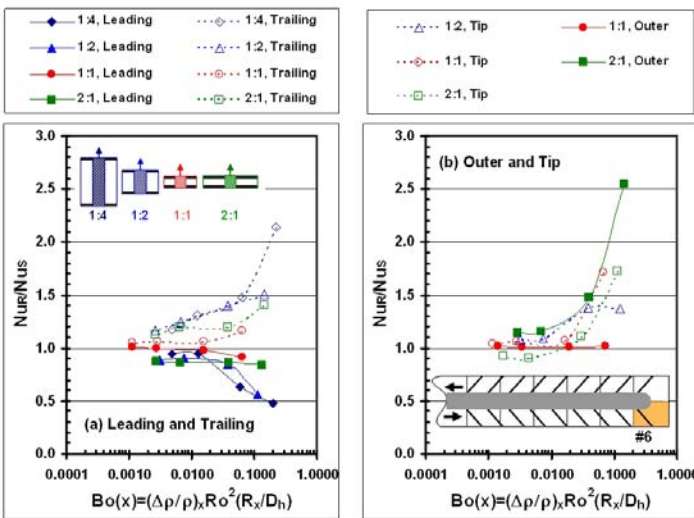


Fig. 28. Nusselt Number Ratio Comparison at Region 6 (1<sup>st</sup> Pass Turn) in Rotating Channels ( $\beta = 90^\circ$ ) with 45° Angled Ribs

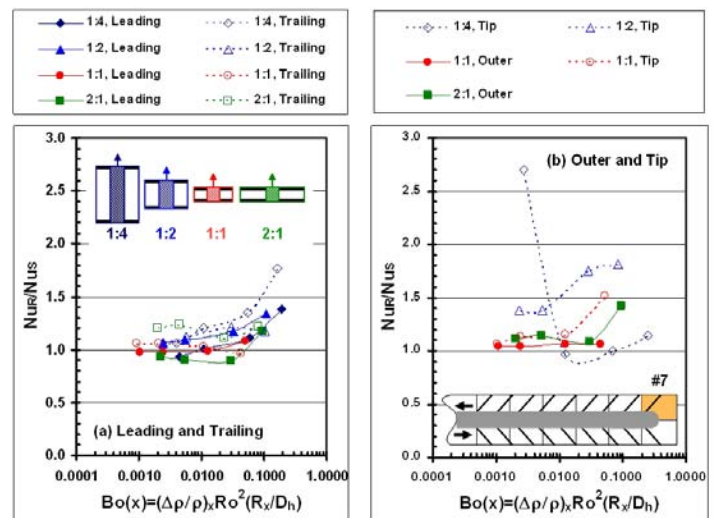


Fig. 29. Nusselt Number Ratio Comparison at Region 7 (2<sup>nd</sup> Pass Turn) in Rotating Channels ( $\beta = 90^\circ$ ) with 45° Angled Ribs

Figures 28 and 29 show the effect of rotation in the turn of the ribbed channels. Similar to region 4, figure 28(a) shows Nusselt number ratios on the trailing surface are increasing with buoyancy parameter, while they decrease on the leading surface; the greatest effect of rotation is seen in the 1:4 channel. Meanwhile, the outer and tip surfaces of each channel are increasing with the increasing effect of rotation. Figure 29 shows in the second half of the turn (region 7), all of the surfaces experience heat transfer enhancement with the increasing buoyancy parameter. The level of enhancement on the outer and tip surfaces is strongly dependent on the channel aspect ratio.

With an understanding of the heat transfer enhancement in orthogonally rotating channels with rib turbulators, the additional complexities in skewed channels with angled ribs can be discussed. Figures 30 – 33 show the Nusselt number ratios in cooling channels with angled ribs with non-orthogonal rotating angles. As with the smooth channels, the 1:4 and 1:2 channels have orientation angles of 45°, the 2:1 and 4:1 channels have orientation angles of 135°, and the 1:1 channels maintains an orientation of 90°. As shown in figure 30, the enhancement due to rotation is less in the skewed channels than the normal channels of region 4. The declination in the Nusselt numbers is significantly less in the channels with skewed orientations than the declination in the normal channels. The orientation of the channel does not significantly effect the heat transfer enhancement on the trailing, inner, or outer surfaces.

The effect of channel orientation on the heat transfer coefficients decreases in the second pass. Figure 31 shows that the trends and level of enhancement on the leading and trailing surfaces of the skewed channels are the same as those of the normal channels. This can be anticipated as the effect of rotation decreases in the second pass, and altering the orientation angle further lessens the effect of rotation on the cooling channel heat transfer coefficients. The diminished effect of rotation is clearly seen on the inner walls of the 1:4 and 2:1 channels. Significant enhancement is seen on the inner wall of the 1:4 channel while extreme declination is seen on the inner wall of the 2:1 channel (figure 27); however, neither of these trends are seen the skewed channels (figure 31).

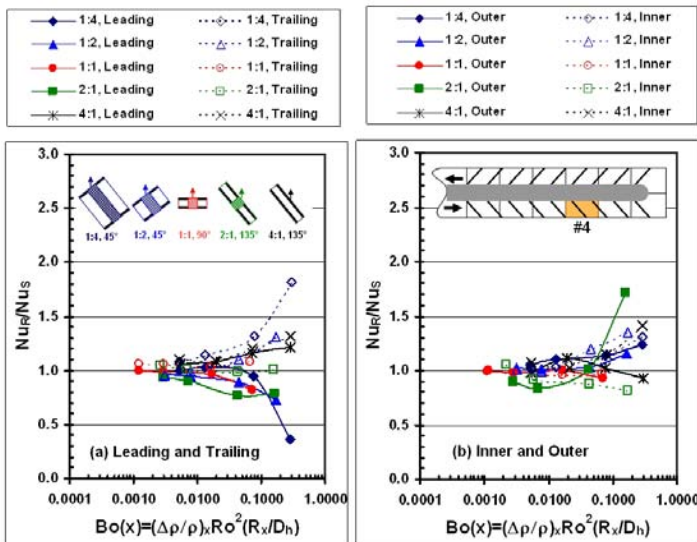


Fig. 30. Nusselt Number Ratio Comparison at Region 4 (1<sup>st</sup> Pass, Fully Developed) in Rotating Channels ( $\beta = 45^\circ$  or  $135^\circ$ ) with  $45^\circ$  Angled Ribs

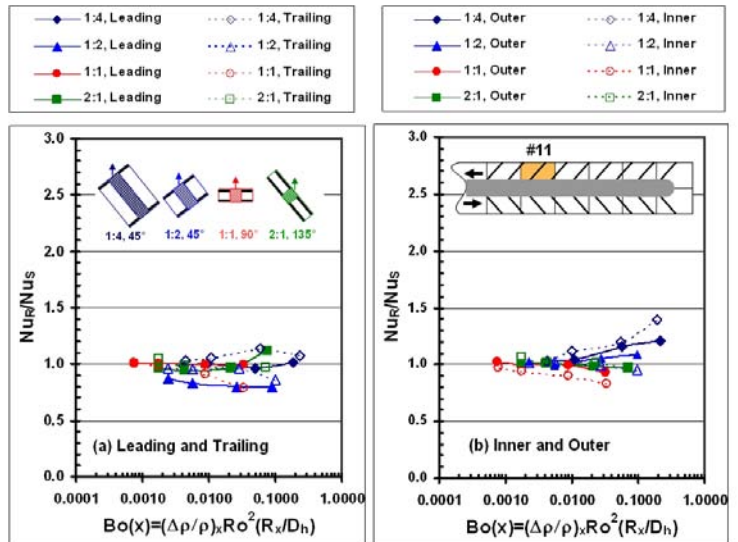


Fig. 31. Nusselt Number Ratio Comparison at Region 11 (2<sup>nd</sup> Pass, Fully Developed) in Rotating Channels ( $\beta = 45^\circ$  or  $135^\circ$ ) with  $45^\circ$  Angled Ribs

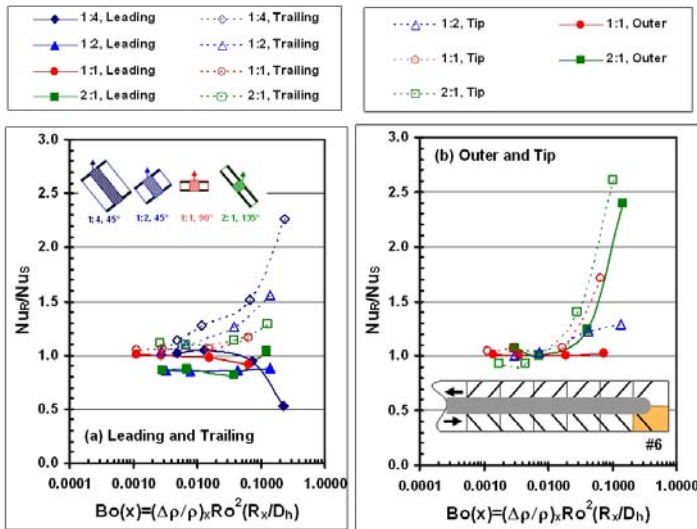


Fig. 32. Nusselt Number Ratio Comparison at Region 6 (1<sup>st</sup> Pass Turn) in Rotating Channels ( $\beta = 45^\circ$  or  $135^\circ$ ) with  $45^\circ$  Angled Ribs

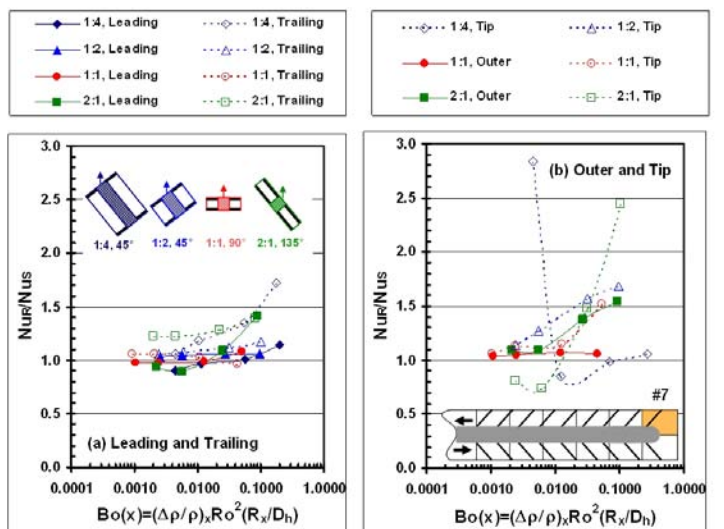


Fig. 33. Nusselt Number Ratio Comparison at Region 7 (2<sup>nd</sup> Pass Turn) in Rotating Channels ( $\beta = 45^\circ$  or  $135^\circ$ ) with  $45^\circ$  Angled Ribs

Similar to the smooth channels, figures 32 and 33 show a minimal effect of channel orientation in the turn of the two pass channels. The leading and trailing surfaces are affected less in the skewed channels than the normal channels in region 6; however in region 7, there is only negligible difference between the Nusselt number ratios on the leading and trailing surfaces. The heat transfer coefficients on the outer and tip surfaces of the 2:1 channel with the  $135^\circ$  orientation are positively influenced by the skewed channel orientation.

The effect of channel orientation is further discussed by considering the average heat transfer enhancement of the two pass channels. Fu et al. presented the overall Nusselt number ratio (measured Nusselt number to the Nusselt number for turbulent flow through a smooth tube, Dittus-Boelter correlation) in two pass smooth and ribbed channels<sup>94</sup>. The overall average Nusselt number ratio was taken as the 12 region average of both the leading and trailing surfaces. Figure 34 shows the effect of rotation is greater in the 1:4 and 1:2 smooth channels than the 1:1 and 2:1 smooth channels. It should be noted that Fu et al. conducted their experiments at constant rotational speed (550 rpm)<sup>95</sup>. Therefore, the rotation number varies inversely with the Reynolds number of the coolant flow. Therefore, the rotation number is the highest at the lowest Reynolds number. Similar to the smooth channels, the effect of rotation is most apparent in the 1:4 channel.

## 4.2.2.2 Enhanced AR Internal Cooling of Turbine Blades and Vanes

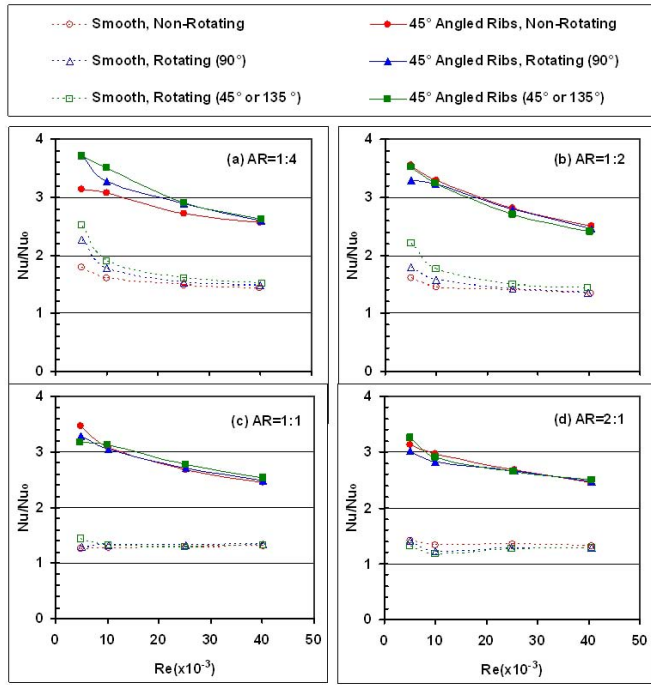


Fig. 34. Channel Averaged Nusselt Number Ratios for Non-Rotating and Rotating Channels

To further evaluate the viability of the various cooling channels, the frictional losses should be considered along with the heat transfer enhancement. Figure 35 shows the friction factor ratios measured by Fu et al. for the various aspect ratio channels<sup>96</sup>. The friction factor ratios in the smooth channels are greater than unity due to the large pressure loss incurred in the 180° turns. The friction factor ratios in the ribbed channels vary significantly depending on the channel aspect ratio. The maximum friction factor is 5.8 in the 1:4 channel, while the friction factor in the 2:1 channel can be 11.5 times greater than the friction factor in a smooth tube as given by the Blasius correlation. Physically the ribs in each of the four channels are the same size. Therefore, the blockage due to the ribs in the 2:1 channel is 5 times greater than the blockage in the 1:4 channel, and at a Reynolds number of 25,000, the increased blockage results in a friction factor ratio increase of 2.3 times. To heat transfer enhancement and the pressure penalty are combined in figure 36 to evaluate the overall thermal performance in each channel. As expected the 1:4 channels have the greatest thermal performance, as they have the lowest friction factor ratios.

### Numerical Simulations of Cooling Channel Heat Transfer Enhancement

Thus far a wide variety of experimental results have been discussed for the enhancement of cooling channel heat transfer. However, numerical predictions have helped researchers better understand the complex flow phenomena in the cooling passages. The  $k-\epsilon$ , low Reynolds  $k-\epsilon$ , the two-layer  $k-\epsilon$ , and the low Reynolds number  $k-\omega$  turbulence models have been used to predict the flow behavior and heat transfer enhancement in rotating cooling channels. However, problems with each of these models can lead to inaccurate predictions of the complex flow in rotating channels. Prakash and Zerkle showed the  $k-\epsilon$  model is unable to predict the flow and heat transfer behavior in two pass rotating channels with angled ribs due to the isotropic turbulence assumption and the near surface wall function required by this model<sup>97</sup>. However, Lin et al. showed the low Reynolds  $k-\omega$  model is an adequate model for rotating two pass cooling channels with angled ribs<sup>98</sup>. This model replaces the wall function in the near wall region with turbulence dissipation specified in terms of the turbulent kinetic energy.

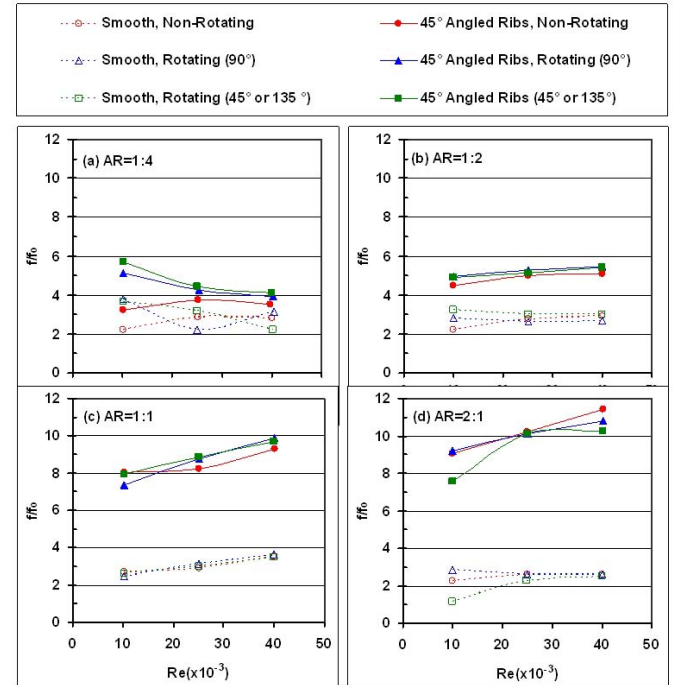


Fig. 35. Overall Friction Factor Ratios for Non-Rotating and Rotating Channels

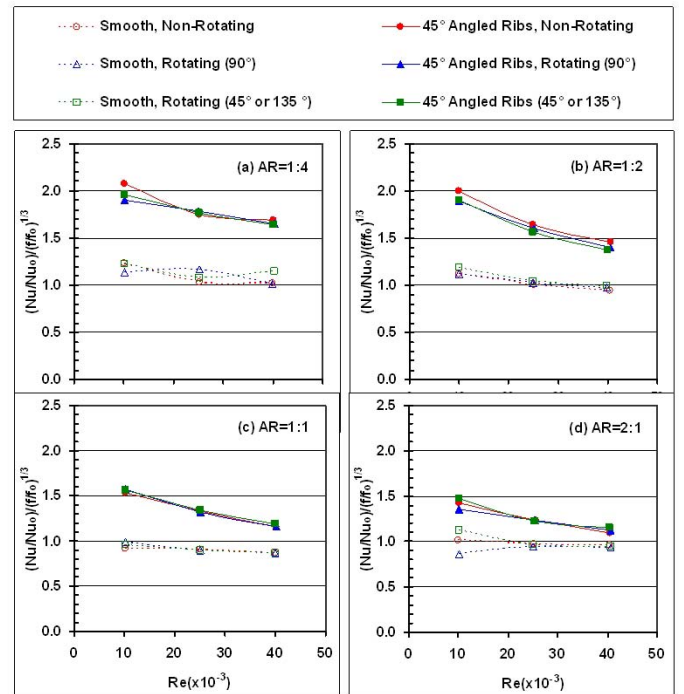


Fig. 36. Overall Thermal Performance for Non-Rotating and Rotating Channels

The advanced Reynolds stress model and the second moment closure model have also been applied to rotating cooling channels. The second moment closure model requires more computing power than the previously mentioned models as six additional transport equations are solved in the three-dimensional turbulent flow field. Also, the eddy diffusivity in the momentum transport equation is replaced with the source terms developed from the turbulent Reynolds stress tensor. At the expense of additional computational time, this model provides accurate predictions for flow in two pass rotating channels with angled rib turbulators.

The second moment closure model used by Chen et al. has been applied to internal cooling channels with a wide range of turbulator configurations and channel aspect ratios<sup>99</sup>. The model was applied to a single pass rotating channel with a square cross-section by Jang et al.<sup>100</sup>. The predicted heat transfer coefficients in channels with either 45° or 60° angled ribs compared favorably with experimental data. Al-Qahtani et al. extended these predictions to include 2:1 two pass channels and 4:1 single pass channels with 45° angled ribs<sup>101</sup>. Su et al. used this same second moment closure model to predict the heat transfer coefficients in rotating 4:1 single pass channels with V-shaped ribs<sup>102</sup>. Figure 37 shows the velocity vectors and temperature contours in non-rotating, single pass 4:1 channels (with angled and V-shaped ribs) and a non-rotating, 2:1 two pass channel with angled ribs. The figures clearly show near the wall, the coolant follows the rib turbulators. The dimensionless temperature contours show the lowest coolant temperatures occur at the most upstream point on the ribs. In addition, the wall temperature is relatively high just downstream of the ribs, due to the flow separation that occurs as the coolant flows over the turbulators.

The secondary flow and temperature contours in a two pass, rotating channel with an aspect ratio of 2:1 is shown in figure 38<sup>103</sup>. In this channel, with smooth walls, the shift of the coolant toward the trailing surface of the first pass is clearly seen. With the core of the coolant forced to the trailing surface, a steep temperature gradient near the trailing wall forms. The thinner boundary layer on this destabilized trailing surface results in enhanced heat transfer coefficients due to rotation. The opposite behavior occurs in the second pass, as the core of the mainstream coolant is forced to the leading surface. However, the temperature contours downstream in the second pass are influenced by the flow through the 180° turn, so the flow is not symmetrical in the channel cross-section.

Similar to the experimental studies which cover a wide range of channel aspect ratios, Su et al. performed a complementary study to numerically predict the heat transfer coefficients in the cooling channels with aspect ratios varying from 1:4 to 4:1<sup>104</sup>. Figure 39 shows the secondary flow and dimensionless temperature contours in the first pass of rotating cooling channels with 45° angled ribs. This study includes parameter variations which are unachievable in most experimental facilities. They found that for the low Reynolds number and low rotation number cases, the rotation effect on the Nusselt number and friction factor ratios is more significant in the 1:2 channel than those observed in either the square or 1:4 channel due to the presence of strong turn-induced vortices. However, in the under engine-like conditions with high rotation and high Reynolds numbers, the effect of rotation decreases as the channel aspect ratio changes from 1:1 to 1:2 and finally to 1:4.

Although the previously mentioned studies are only a sampling of those utilizing the second moment turbulence model, they have demonstrated the power of this advanced second-order Reynolds stress turbulence model. The models have been validated with existing experimental data, and upon validation, they have been extended to high Reynolds number and high rotation number flows which cannot be obtained in most experimental facilities. Over a wide range of flow conditions, these predictions provide detailed velocity, pressure, and temperature profiles which are essential to understanding the complex flow behavior in these rotating channels.

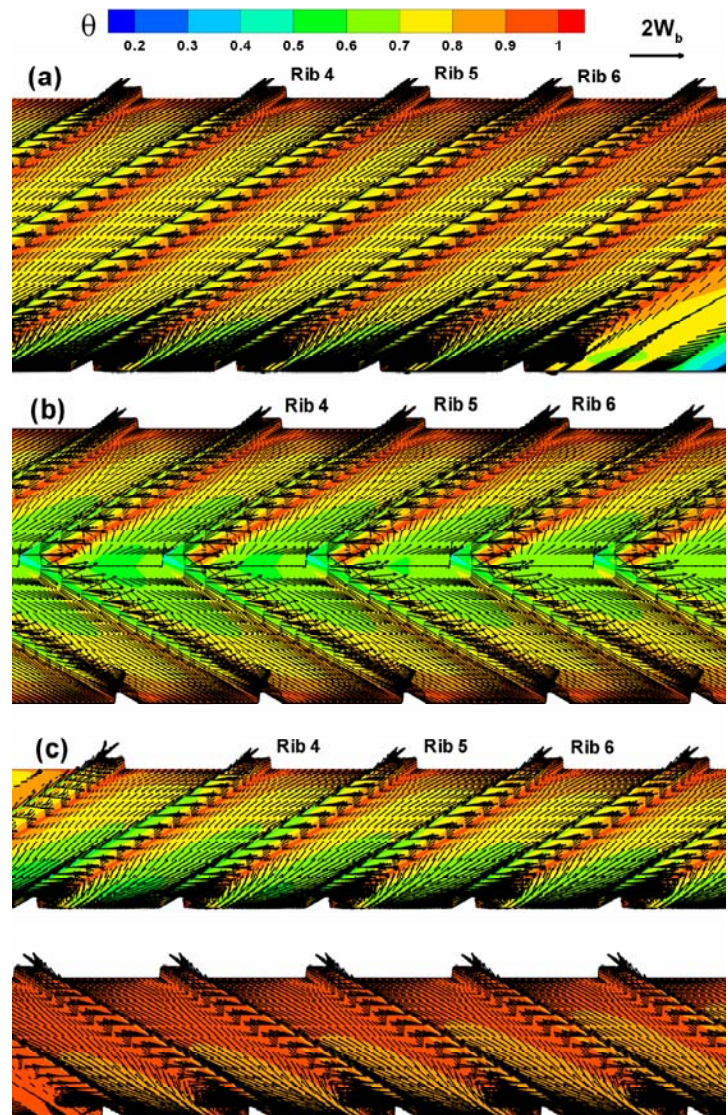


Fig. 37. Velocity Vectors and Temperature Contours: (a) AR = 4:1 One-pass Channel with 45° Inclined Ribs, (b) AR = 4:1 One Pass Channel with V-shaped Ribs, (c) AR = 2:1 Two-Pass Channel with 45° Inclined Ribs (Re = 10,000)

## 4.2.2.2 Enhanced Internal Cooling of Turbine Blades and Vanes

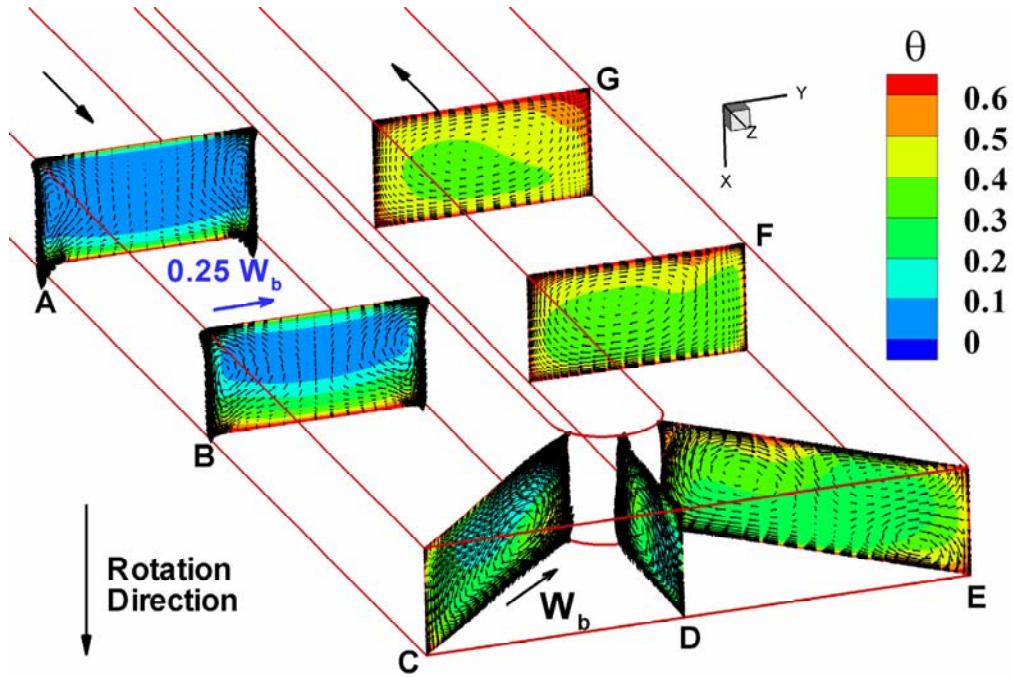


Fig. 38. Secondary Flow and Temperature Contours in Rotating AR = 2:1 Smooth Duct ( $Re = 10,000$ ,  $Ro = 0.22$ )

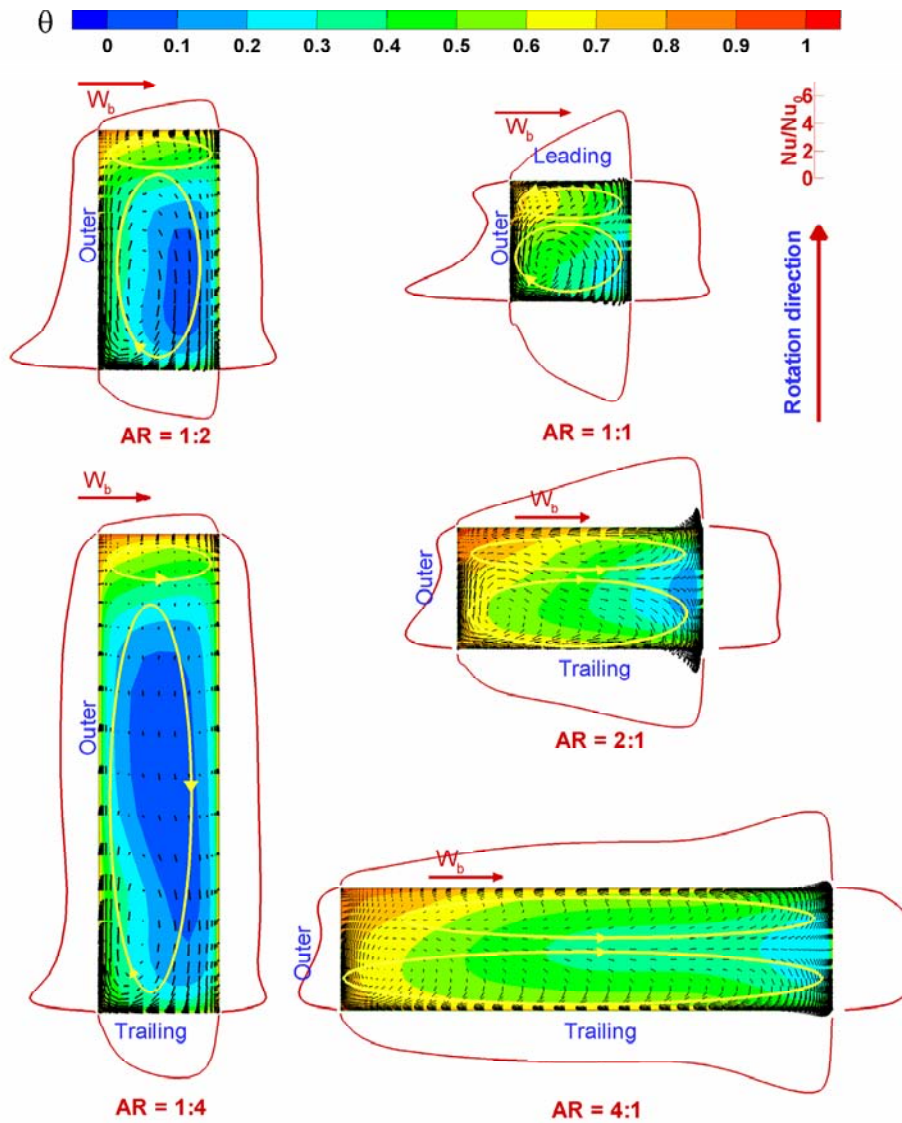


Fig. 39. A Secondary Flow in the First Passage (before the  $180^\circ$  turn) of Rotating Ribbed Channels with Different Aspect Ratios ( $Re = 10,000$ ,  $Ro = 0.14$ )



### ***Flow Field Measurements in Rotating Cooling Channels***

Heat transfer is a side effect of the flow field. Flow in a rotating channel is significantly different from flow in a non-rotating channel. The secondary flow in rotation redistributes velocity and also alters the random velocity fluctuation patterns in turbulent flows. Lezius and Johnston examined flow instability in a straight rectangular channel with smooth walls caused by rotation<sup>105</sup>. They reported that rotation increases flow velocity and turbulence near the unstable trailing wall and reduces the turbulent fluctuations significantly near the stable leading wall. Elfert measured velocity and turbulence distributions in a rotating circular pipe<sup>106</sup>. Rotation shifts the bulk flow toward the trailing side, and the turbulence profile shows a different distribution due to rotation. Tse and Mcgrath used laser-Doppler velocimetry to measure rotating flow in a two-pass channel with smooth and ribbed walls<sup>107</sup>. Tse and Steuber investigated the mean flow characteristics in the first and second passages of a rotating four-pass coolant passage with 45° ribs of semi-circular cross section using LDA<sup>108</sup>. Cheah et al. used the LDA to measure the velocity and turbulence quantities in a rotating two-pass channel<sup>109</sup>. Bons and Kerrebrock measured the internal flow in a straight smooth-wall channel with particle image velocimetry (PIV) for both heated and non-heated cases<sup>110</sup>. Schabacker et al. and Chanteloup et al. also used PIV to measure the flows in stationary two-pass square ducts with 45° turbulators<sup>111</sup>. Son et al. measured the flows in two-pass channels with smooth and 90° ribbed walls using PIV<sup>112</sup>. Liou and Chen measured the developing flow in a two-pass channel with LDA<sup>113</sup>. Liou et al. studied fluid flow in a rotating two-pass duct with in-line 90° ribs using LDA<sup>114</sup>. Liou et al. also performed LDV and pressure measurements for in-line detached 90° ribs<sup>115</sup>. Liou and Dai measured pressure and flow characteristics in a rotating two-pass square duct with 45° angled ribs of square cross section by using the LDA<sup>116</sup>. Liou et al. measured flow and pressure fields in a rotating two-pass duct with staggered 45° ribs of rounded cross section<sup>117</sup>. Both Liou and Dai and Liou et al. reported that the absence of periodic fully developed flow condition in their tests<sup>118</sup>. The above-mentioned flow measurements help to understand the flow physics and serve to explain the heat transfer results obtained in two-pass rotating channels with smooth and ribbed walls.

### ***Rotational Effect on Jet Impingement Cooling***

Several studies were mentioned above that investigate jet impingement cooling. Although a number of impingement studies have been completed, only a few studies consider the effect of rotation on impingement cooling. Epstein et al. studied the effect of rotation on impingement cooling in the leading edge of a blade<sup>119</sup>. They reported that the rotation decreases the impingement heat transfer, but the effective heat transfer is better than a smooth rotating channel. The zero staggered cooling jets (i.e., jet direction is perpendicular to rotation direction) show lower heat transfer coefficients compared to that with a staggered angle. Mattern and Hennecke reported the effect of rotation on the leading edge impingement cooling by using the naphthalene sublimation technique<sup>120</sup>. Their experiment did not include the rotating buoyancy effect. The jet direction has an offset angle with respect to the rotation direction. They found that the rotation decreases the impingement heat transfer for all staggered angles. The effect of rotation is least when jet direction has an angle of 45° to rotation direction. However, a maximum of 40% reduction in heat transfer is noted when jet direction is perpendicular to rotation direction. This may be because the Coriolis force creates a swirl action on the spent flow and also deflects the jet when jet direction is parallel to rotation direction. Glezer et al. studied the effect of rotation on swirling impingement cooling in the leading edge of a blade<sup>121</sup>. They found that screw-shaped swirl cooling can significantly improve the heat-transfer coefficient over a smooth channel and the improvement is not significantly dependent on the temperature ratio and rotational forces.

Parsons et al. studied the effect of rotation on impingement cooling in the mid-chord region of the blade<sup>122</sup>. A central chamber serves as the pressure chamber, and jets are released in either direction to impinge on two heated surfaces. The jet impinging directions have different orientations with respect to the direction of rotation. They reported that the rotation decreases the impingement heat transfer on both leading and trailing surfaces with more effect on the trailing side (up to 20% heat transfer reduction). Akella and Han studied the effect of rotation on impingement cooling for a two-pass impingement channel configuration with smooth walls<sup>123</sup>. The difference from the earlier experiment by Parsons et al. is that spent jets from the trailing channel are used as cooling jets for the leading channel<sup>124</sup>. Therefore, the cross-flow in the trailing side is radial outward; for the leading side, it is radial inward. They reported that irrespective of the direction of rotation, the heat transfer coefficient on the first-pass and second-pass impinging wall decreases up to 20% in the presence of rotation. Akella and Han included 45° angled ribs in the target surfaces of their two-pass impingement channel with rotation<sup>125</sup>. They reported that jet impingement on the ribbed wall can provide 10-50% more heat transfer compared to that on the smooth wall for jet Reynolds number increasing from 4,000 to 10,000. This is because the angled rib-induced secondary flow gets stronger with higher cross-flow at higher jet Reynolds number. They also found that the rotation decreases impingement heat transfer on the first-pass and second-pass ribbed wall. Parsons et al. extended their earlier work to include heat transfer on a smooth target wall with film coolant extraction from a channel with four heated walls<sup>126</sup>.

### ***Rotational Effect on Pin-Fin Cooling***

Pin-fin cooling has been investigated for many years, but only recently has the effect of rotation been considered in channels with pin-fins. Recently, Willett and Bergles studied the effect of rotation on heat transfer in narrow rectangular channels (AR = 10:1) with smooth and with typical pin-fin array, respectively, including channel orientation effect with respect to the plane of rotation<sup>127</sup>. They found that the heat transfer enhancement in the pin-fin channel due to rotation and buoyancy was less than the enhancement in the smooth channel. They showed that heat transfer enhancement mainly is due to pin-fin flow disturbance; pin-fins significantly reduce the effect of

## 4.2.2.2 Enhanced Internal Cooling of Turbine Blades and Vanes

rotation, but they do not eliminate the effect. Wright et al. studied the effect of rotation on heat transfer in narrow rectangular channels ( $AR = 4:1$  and  $8:1$ ) with typical pin-fin array used in turbine blade trailing edge design and oriented at  $150^\circ$  with respect to the plane of rotation<sup>128</sup>. Results show that turbulent heat transfer in a stationary pin-fin channel can be enhanced up to 3.8 times that of a smooth channel; rotation enhances the heat transferred from the pin-fin channels up to 1.5 times that of the stationary pin-fin channels. Most importantly, for narrow rectangular pin-fin channels oriented at  $150^\circ$  with respect to the plane of rotation, heat transfer enhancement on both the leading and trailing surfaces increases with rotation. This provides positive information for the cooling designers.

### *Rotational Effect on Dimple Cooling*

Because dimple cooling has only recently been considered as an internal cooling technique, the number of studies available in open literature is limited. The majority of dimple studies were described above, and they are only applicable for stator cooling designs. Only a few studies focus on rotor blade dimple cooling. Zhou et al. studied heat/mass transfer in a rotating square channel with typical dimple array<sup>129</sup>. They found that heat transfer enhancement for the stationary dimple channel is around two times that of the smooth wall value; however, rotation enhances heat transfer on the trailing dimple surface and reduces heat transfer on the leading dimple surface in a similar manner as the rotational effect on the trailing and leading surfaces of the square channel with ribs. Griffith et al. studied heat transfer in rotating rectangular channels ( $AR = 4:1$ ) with typical dimple array on both leading and trailing walls, including the effect of channel orientation with respect to the plane of rotation<sup>130</sup>. The results show that rotation enhances heat transfer on both trailing and leading surfaces of the narrow dimpled channel in a similar trend as the rotational effect on the trailing and leading surfaces of the narrow rectangular channel with ribs or pins; however, the heat transfer enhancement of the ribbed or pinned channel exceeds that of the dimpled channel. Also, the dimpled channel oriented at  $135^\circ$  with respect to the plane of rotation provides greater overall heat transfer enhancement than the orthogonal dimpled channel.

### 4.2.2.2-4 Concluding Remarks

With modern gas turbines operating at extremely high temperatures, it is necessary to implement various cooling methods, so the turbine blades and vanes survive in the path of the hot gases. Simply passing coolant air through the airfoils does not provide adequate cooling; therefore, it is necessary to implement techniques that will further enhance the heat transfer from the airfoil walls. The internal heat transfer can be enhanced with jet impingement, pin-fin cooling (used in the trailing edge), and internal passages lined with turbulence promoters. The most commonly used turbulators are ribs. The heat transfer distribution in cooling channels with ribs has been studied for many years because a number of factors combine to affect the heat transfer. Because the flow through non-rotating and rotating channels is very different, many studies have focused on the effect of rotation in ribbed channels. Although the majority of studies concentrate on channels with a square cross-section, a limited number of investigations are now available for rectangular cooling channels with ribs. A relatively new alternative to rib turbulators are dimples. A limited number of studies are available to address the heat transfer in stationary channels with dimples, and even fewer studies are available that address the effect of rotation in cooling channels with dimples. It is also important to investigate the effect of rotation on jet impingement and pin-fin cooling, and in the recent years, such studies have become available.

More studies are needed for the blade-shaped coolant passages with high performance turbulators and with or without film cooling holes under realistic coolant flow, thermal, and rotating conditions. Also, more studies are needed for rotating impingement cooling with or without film coolant extraction as well as rotating pin-fin cooling with or without trailing edge ejection in order to guide the efficient rotor blade internal cooling designs. Highly accurate and highly detailed local heat transfer data is needed to aid engineers in their design of blades for advanced gas turbines.

## 4.2.2.2-5 Notes

1. J.C. Han, S. Dutta, and S.V. Ekkad, “*Gas Turbine Heat Transfer and Cooling Technology*,” Taylor & Francis, Inc., New York, New York, December 2000, ISBN # 1-56032-841-X, 646 pages.
2. B. Lakshminryana, “Turbine Cooling and Heat Transfer,” *Fluid Dynamics and Heat Transfer of Turbomachinery*, John Wiley, New York, 1996, pp. 597-721; M.G. Dunn, “Convection Heat Transfer and Aerodynamics in Axial Flow Turbines,” *ASME Journal of Turbomachinery*. 123 no.4 (2001): 637-686.
3. R.J. Goldstein, “Heat Transfer in Gas Turbine Systems,” *Annals of The New York Academy of Sciences*, New York, New York, Vol. 934, 2001, 2001, 520 pages.
4. D.E. Metzger, L.W. Florschuetz, D.I. Takeuchi, R.D. Behee, and R.A. Berry, “Heat Transfer Characteristics for Inline and Staggered Arrays of Circular Jets with Crossflow of Spent Air,” *ASME Journal of Heat Transfer*, 101 (1979): 526-531.
5. L.W. Florschuetz, R.A. Berry, and D.E. Metzger, “Periodic Streamwise Variations of Heat Transfer Coefficients for Inline and Staggered Arrays of Circular Jets with Crossflow of Spent Air,” *ASME Journal of Heat Transfer* 102 (1980): 132-137; R.N. Koopman and E.M. Sparrow, “Local and Average Transfer Coefficients Due to an Impinging Row of Jets,” *International Journal of Heat and Mass Transfer* 92 (1976): 73-82.
6. L.W. Florschuetz and C.C. Su, “Effects of Crossflow Temperature on Heat Transfer Within an Array of Impinging Jets,” *ASME Journal of Heat Transfer* 109 (1987): 74-82.
7. Ibid.
8. D.M. Kercher and W. Tabakoff, “Heat Transfer by a Square Array of Round Air Jets Impinging Perpendicular to a Flat Surface Including the Effect of Spent Air,” *ASME Journal of Engineering for Power*, Vol. 92 (1970): 73-82; L.W. Florschuetz, C.R. Truman, and D.E. Metzger, “Streamwise Flow and Heat Transfer Distributions for Jet Array Impingement with Crossflow,” *ASME Journal of Heat Transfer* 103 (1981): 337-342.
9. See note 8 (Florschuetz, et al.).
10. J.C. Bailey and R.S. Bunker, “Local Heat Transfer and Flow Distributions for Impinging Jet Arrays of Dense and Sparse Extent,” ASME Paper No. GT-2002-30473 (2002); also see note 8 (Florschuetz, et al.).
11. Y. Huang, S.V. Ekkad, and J.C. Han, “Detailed Heat Transfer Distributions Under an Array of Orthogonal Impinging Jets,” *AIAA Journal of Thermophysics and Heat Transfer* 12 (1998): pp. 73-79.
12. S.V. Ekkad, Y. Huang, and J.C. Han, “Impingement Heat Transfer on a Target Plate with Film Holes,” *AIAA Journal of Thermophysics and Heat Transfer* 13 (1999): 522-528.
13. T. Wang, M. Lin, and R.S. Bunker, “Flow and Heat Transfer of Confined Impingement Jets Cooling,” ASME Paper No. 2000-GT-223 (2000).
14. L. Gao, S.V. Ekkad, and R.S. Bunker, “Impingement Heat Transfer Under Linearly Stretched Arrays of Holes,” ASME Paper No. GT2003-38178 (2003).
15. L.W. Florschuetz, D.E. Metzger, and C.C. Su, “Heat Transfer Characteristics for Jet Array Impingement with Initial Crossflow,” *ASME Journal of Heat Transfer* 106 (1984): pp. 34-41.
16. R.E. Chupp, H.E. Helms, P.W. McFadden, and T.R. Brown, “Evaluation of Internal Heat Transfer Coefficients for Impingement Cooled Turbine Airfoils,” *AIAA Journal of Aircraft*. 6 (1969): 203-208.
17. R.S. Bunker and D.E. Metzger, “Local Heat Transfer in Internally Cooled Turbine Airfoil Leading Edge Regions. Part I: Impingement Cooling Without Film Coolant Extraction,” *ASME Journal of Turbomachinery* 112 (1990): 451-458.
18. D.E. Metzger and R.S. Bunker, “Local Heat Transfer in Internally Cooled Turbine Airfoil Leading Edge Regions. Part II: Impingement Cooling with Film Coolant Extraction,” *ASME Journal of Turbomachinery*. 112 (1990): 459-466.
19. D.E. Metzger, R.A. Berry, and J.P. Bronson, “Developing Heat Transfer in Rectangular Ducts With Staggered Arrays of Short Pin Fins,” *ASME Journal of Heat Transfer* 104 (1982): 700-706.
20. M.K. Chyu, Y.C. Hsing, T.I.P. Shih, and V. Natarajan, “Heat Transfer Contributions of Pins and Endwall in Pin-Fin Arrays: Effects of Thermal Boundary Condition Modeling,” ASME Paper No. 98-GT-175 (1998).
21. VanFossen, G.J., 1982, “Heat-Transfer Coefficients for Staggered Arrays of Short Pin Fins,” *ASME Journal of Engineering for Power*, Vol. 104, pp. 268-274; also see note 19.
22. S.C. Arora and W. Abdel-Messeh, “Characteristics of Partial Length Circular Pin Fins as Heat Transfer Augmentors for Airfoil Internal Cooling Passages,” ASME Paper No. 89-GT-87 (1989).
23. D.E. Metzger, S.C. Fan, and S.W. Haley, “Effects of Pin Shape and Array Orientation on Heat Transfer and Pressure Loss in Pin Fin Arrays,” *ASME Journal of Engineering for Gas Turbines and Power* 106 (1984): 252-257.
24. M.K. Chyu, “Heat Transfer and Pressure Drop for Short Pin-Fin Arrays With Pin-Endwall Fillet,” *ASME Journal of Heat Transfer* 112 (1990): 926-932.
25. R.J. Goldstein, M.Y. Jabbari, and S.B. Chen, “Convective Mass Transfer and Pressure Loss Characteristics of Staggered Short Pin-Fin Arrays,” *International Journal of Heat and Mass Transfer* 37 (1994): Suppl. 1, pp. 149-160.
26. M.K. Chyu, Y.C. Hsing, and V. Natarajan, “Convective Heat Transfer of Cubic Fin Arrays in a Narrow Channel,” *ASME Journal of Turbomachinery* 120 (1998): 362-367.

## 4.2.2.2 Enhanced Internal Cooling of Turbine Blades and Vanes

27. D.E. Metzger, W.B. Shephard, and S.W. Haley, "Row Resolved Heat Transfer Variations in Pin-Fin Arrays Including Effects of Non-Uniform Arrays and Flow Convergence," ASME Paper No. 86-GT-132 (1986).
28. M.K. Chyu, V. Natarajan, and D.E. Metzger, "Heat/Mass Transfer from Pin-Fin Arrays With Perpendicular Flow Entry," ASME HTD-Vol. 226 (1992), Fundamentals and Applied Heat Transfer Research for Gas Turbine Engines.
29. T.K. Kumaran, J.C. Han, and S.C. Lau, "Augmented Heat Transfer in a Pin Fin Channel with Short or Long Ejection Holes," *International Journal of Heat Mass Transfer*, 34 no. 10 (1991): 2617-2628.
30. Hwang, J.J. and Lu, C.C., 2000, "Lateral-Flow Effect of Endwall Heat Transfer and Pressure Drop in a Pin-Fin Trapezoidal Duct of Various Pin Shapes," ASME Paper No. 2000-GT-0232.
31. M.K. Chyu, Y. Yu, H. Ding, J.P. Downs, and O. Soechting, "Concavity Enhanced Heat Transfer in an Internal Cooling Passage," ASME Paper No. 97-GT-437 (1997); H.K. Moon, T. O'Connell, and B. Glezer, "Channel Height Effect on Heat Transfer and Friction in a Dimpled Passage," ASME Paper No. 99-GT-163 (1999); G.I. Mahmood, M.L. Hill, D.L. Nelson, P.M. Ligrani, H.K. Moon, and B. Glezer, "Local Heat Transfer and Flow Structure on and above a Dimpled Surface in a Channel," *ASME Journal of Turbomachinery* 123 (2001): 115-123; S.W. Moon, and S.C. Lau, "Turbulent Heat Transfer Measurements on a Wall with Concave and Cylindrical Dimples in a Square Channel," ASME Paper No. GT-2002-30208 (2002).
32. R.S. Bunker and K.F. Donnellan, "Heat Transfer and Friction Factors for Flows Inside Circular Tubes with Concavity Surfaces," ASME Paper No. GT-2003-38053 (2003).
33. N. Syred, A. Khalatov, A. Kozlov, A. Shchukin, and R. Agachev, "Effect of Surface Curvature on Heat Transfer and Hydrodynamics within a Single Hemispherical Dimple," ASME Paper No. 2000-GT-236 (2000).
34. G.M.S. Azad, Y. Huang, and J.C. Han, "Jet Impingement Heat Transfer on Dimpled Surfaces Using a Transient Liquid Crystal Technique," *ALAA Journal of Thermophysics and Heat Transfer* 14 no. 2 (2000): 186-193; G.M.S. Azad, Y. Huang, and J.C. Han, "Impingement Heat Transfer on Pinned Surfaces Using a Transient Liquid Crystal Technique," Proceedings of the 8<sup>th</sup> International Symposium on Transport Phenomena and Dynamics of Rotating Machinery 2 (2000): 731-738.
35. M.E. Taslim, L. Setayeshgar, and S.D. Spring, "An Experimental Evaluation of Advanced Leading Edge Impingement Cooling Concepts," ASME Paper No. 2000-GT-222 (2000).
36. M.E. Taslim, Y. Pan, and S.D. Spring, "An Experimental Study of Impingement on Roughened Airfoil Leading-Edge Wall with Film Holes," ASME Paper No. 2001-GT-0152 (2001).
37. M.E. Taslim and L. Setayeshgar, "Experimental Leading-Edge Impingement Cooling Through Racetrack Crossover Holes," ASME Paper No. 2001-GT-153 (2001); M.E. Taslim, Y. Pan, and K. Bakhtari, "Experimental Racetrack Shaped Jet Impingement on a Roughened Leading-Edge Wall with Film Holes," ASME Paper No. GT-2002-30477(2002).
38. B. Glezer, H.K. Moon, J. Kerrebrock, J. Bons, and G. Guenette, "Heat Transfer in a Rotating Radial Channel With Swirling Internal Flow," presented at the International Gas Turbine & Aeroengine Congress and Exhibition, Stockholm, Sweden, June 2-5, ASME Paper No. 98-GT-214 (1998).
39. G. Pamula, S.V. Ekkad, and S. Acharya, "Influence of Cross-Flow Induced Swirl and Impingement on Heat Transfer in a Two-Pass Channel Connected by Two Rows of Holes," ASME Paper No. 2000-GT-235 (2000).
40. S. Kieda, T. Torii, and K. Fujie, "Heat Transfer Enhancement in a Twisted Tube Having a Rectangular Cross Section With or Without Internal Ribs," ASME Paper No. 84-HT-75 (1984).
41. Y.M. Zhang, G.M.S. Azad, J.C. Han, and C.P. Lee, "Heat Transfer and Friction Characteristics of Turbulent Flow in Square Ducts with Wavy, and Twisted Tape Inserts and Axial Interrupted Ribs," *Journal of Enhanced Heat Transfer* 7 (2000): 35-49.
42. Y.M. Zhang, W.Z. Gu, and J.C. Han, "Heat Transfer and Friction in Rectangular Channels With Ribbed or Ribbed-Grooved Walls," *ASME Journal of Heat Transfer* 116 no. 1 (1994): 58-65.
43. D.E. Metzger and C.S. Fan, "Heat Transfer in Pin-Fin Arrays With Jet Supply and Large Alternating Wall Roughness Ribs," HTD-Vol. 226 (1992) Fundamental and Applied Heat Transfer Research for Gas Turbine Engines, pp. 23-30.
44. Z.J. Zuo, A. Faghri, and L. Langston, "A Parametric Study of Heat Pipe Turbine Vane Cooling," presented at the International Gas Turbine and Aeroengine Congress and Exhibition, Orlando, Florida, June 2-5, ASME Paper No. 97-GT-443 (1997).
45. S. Yamawaki, T. Yoshida, M. Taki, and F. Mimura, "Fundamental Heat Transfer Experiments of Heat Pipes for Turbine Cooling," ASME Paper No. 97-GT-438 (1997).
46. J.L. Kerrebrock and D.B. Stickler, "Vaporization Cooling for Gas Turbines, the Return-Flow Cascade," ASME Paper No. 98-GT-177 (1998).
47. G.B. Bruening and W.C. Chang, "Cooled Cooling Air Systems for Turbine Thermal Management," ASME Paper No. 99-GT-14 (1999).
48. J.C. Corman and T.C. Paul, "Power Systems for the 21<sup>st</sup> Century "H" Gas Turbine Combined Cycles," GE Power Systems, Schenectady, New York, GER-3935 (1995): 1-12.
49. T. Guo, T. Wang, and J.L. Gaddis, "Mist/Steam Cooling in a Heated Horizontal Tube, Part 2: Results and Modeling," ASME Paper No. 99-GT-145 (1999).
50. X. Li, J.L. Gaddis, and T. Wang, "Mist/Steam Heat Transfer in Confined Slot Jet Impingement," ASME Paper No. 2000-

- GT-0221(2000); X. Li, J.L. Gaddis, and T. Wang, "Mist/Steam Cooling by a Row of Impinging Jets," ASME Paper No. 2001-GT-0151(2001); X. Li, J.L. Gaddis, and T. Wang, "Mist/Steam Heat Transfer with Jet Impingement onto a Concave Surface," ASME Paper No. GT-2002-30475(2002).
51. J.C. Han, L.R. Glicksman, and W.M. Rohsenow, "An Investigation of Heat Transfer and Friction for Rib-Roughened Surfaces," *International Journal of Heat and Mass Transfer* 21 (1978): 1143-1156; J.C. Han, J.S. Park, and C.K. Lei, "Heat Transfer Enhancement in Channels with Turbulence Promoters," *ASME Journal of Engineering for Gas Turbines and Power* 107 (1985): 628-635; J.C. Han, "Heat Transfer and Friction Characteristics in Rectangular Channels with Rib Turbulators," *ASME Journal of Heat Transfer* 110 (1988): 321-328; J.C. Han and J.S. Park, "Developing Heat Transfer in Rectangular Channels with Rib Turbulators," *International Journal of Heat and Mass Transfer* 31(1988): 183-195.
  52. See note 51 (Han [1988]) and (Han & Park [1988]).
  53. J.C. Han, Y.M. Zhang, and C.P. Lee, "Augmented Heat Transfer in Square Channels with Parallel, Crossed, and V-shaped Angled Ribs," *Journal of Heat Transfer, Transactions ASME* 113 (1991): 590-596; J.C. Han and Y.M. Zhang, "High Performance Heat Transfer Ducts with Parallel and V-Shaped Broken Ribs," *International Journal of Heat and Mass Transfer* 35 (1992): 513-523; S.V. Ekkad and J.C. Han, "Detailed Heat Transfer Distributions in Two-Pass Square Channels with Rib Turbulators," *International Journal of Heat and Mass Transfer* 40 (1997): 2525-2537; S.V. Ekkad, Y. Yuang, and J.C. Han, "Detailed Heat Transfer Distributions in Two-Pass Smooth and Turbulated Square Channels with Bleed Holes," *International Journal of Heat and Mass Transfer* 41 (1998):, 3781-3791.
  54. S.C. Lau, R.T. Kukreja, and R.D. McMillin, "Effects of V-shaped Rib Arrays on Turbulent Heat Transfer and Friction of Fully Developed Flow in a Square Channel," *International Journal of Heat and Mass Transfer* 34 (1991): 1605-1616.; M.E. Taslim, T. Li, and D.M. Kercher, "Experimental Heat Transfer and Friction in Channels Roughened with Angled, V-Shaped, and Discrete Ribs on Two Opposite Walls," *ASME Journal of Turbomachinery*, 118 (1996): 20-28; X. Gao and B. Suden, "Heat Transfer and Pressure Drop Measurements in Rib-roughened Rectangular Ducts," *Experimental Thermal and Fluid Science* 24 (2001): 25-34; D.H. Rhee, D.H. Lee, H.H. Cho, and H.K. Moon, "Effects of Duct Aspect Ratios on Heat /Mass Transfer with Discrete V-Shaped Ribs," ASME Paper No. GT2003-38622(2003).
  55. H.H. Cho, S.J. Wu, and H.J. Kwon, "Local Heat/Mass Transfer Measurements in a Rectangular Duct with Discrete Ribs," *ASME Journal of Turbomachinery* 122 (2000): 579-586; also see note 54 (Rhee, et al.).
  56. See note 53 (Han & Zhang).
  57. J.C. Han, J.J. Huang, and C.P. Lee, "Augmented Heat Transfer in Square Channels with Wedge-Shaped and Delta-Shaped Turbulence Promoters," *Journal of Enhanced Heat Transfer* 1 no.1 (1993): 37-52.
  58. R.S Bunker and S.J. Osgood, "The Effect of Turbulator Lean on Heat Transfer and Friction in a Square Channel," ASME Paper No. GT-2003-38137 (2003).
  59. M.E. Taslim and S.D. Spring, "Effects of Turbulator Profile and Spacing on Heat Transfer and Friction in a Channel," *AIAA Journal of Thermophysics and Heat Transfer* 8 no. 3 (1994): 555-562.
  60. J.C. Bailey and R.S. Bunker, "Heat Transfer and Friction in Channels with Very High Blockage 45° Staggered Turbulators," ASME Paper No. GT-2003-38611(2003); M.E. Taslim and S.D. Spring, "Experimental Heat Transfer and Friction Factors in Turbulated Cooling Passages of Different Aspect Ratios where Turbulators are Staggered," AIAA Paper No. 88-3014, 24<sup>th</sup> Joint Propulsion Conference (1988).
  61. J.R. Shen, Z. Wang, P.T. Ireland, T.V. Jones, and A.R. Byerley, "Heat Transfer Enhancement Within a Turbine Blade Cooling Passage Using Ribs and Combinations of Ribs With Film Cooling Holes," *ASME Journal of Turbomachinery* 188 (1996): 428-433; D. Thurman and P. Poinsette, "Experimental Heat Transfer and Bulk Air Temperature Measurements for a Multipass Internal Cooling Model with Ribs and Bleed," ASME Paper No. 2000-GT-233 (2000); also see note 53 (Ekkad, Huang, and Han).
  62. See note 53 (Ekkad, Huang, and Han).
  63. See note 61 (Shen, et al.).
  64. J.H. Wagner, B.V. Johnson, and F.C. Kopper, "Heat Transfer in Rotating Serpentine Passages With Smooth Walls," *ASME Journal of Turbomachinery* 113 (1991): 321-330; S. Dutta and J.C. Han, "Rotational Effects on the Turbine Blade Coolant Passage Heat Transfer," *Annual Review of Heat Transfer* 9 (1997): 269-314.
  65. J.C. Han, Y.M. Zhang, and K. Kalkuehler, "Uneven Wall Temperature Effect on Local Heat Transfer in a Rotating Two-Pass Square Channel with Smooth Walls," *ASME Journal of Heat Transfer* 114 (1993): 850-858.
  66. Ibid.
  67. J.A. Parsons, J.C. Han, and Y.M. Zhang, "Wall Heating Effect on Local Heat Transfer in a Rotating Two-Pass Square Channel with 90-Degree Rib Turbulators," *International Journal of Heat and Mass Transfer* 37 no. 9 (1994): 1411-1420; Y.M. Zhang, J.C. Han, J.A. Parsons, and C.P. Lee, "Surface Heating Effect on Local Heat Transfer in a Rotating Two-Pass Square Channel with 60-Degree Angled Rib Turbulators," *ASME Journal of Turbomachinery* 117 (1995): 272-278.
  68. S. Acharya, V. Eliades, and D.E. Nikitopoulos, "Heat Transfer Enhancements in Rotating Two-Pass Coolant Channels with Profiled Ribs: Part 1 – Average Results," ASME Paper No. 2000-GT-0227 (2000).
  69. J.H. Wagner, B.V. Johnson, R.A. Graziani, and F.C. Yeh, "Heat Transfer in Rotating Serpentine Passages With Trips Normal to the Flow," *ASME Journal of Turbomachinery* 114 (1992): 847-857.
  70. B.V. Johnson, J.H. Wagner, G.D. Steuber, and F.C. Yeh, "Heat Transfer in Rotating Serpentine Passages with Trips Skewed to the Flow," ASME Paper No. 92-GT-191, *ASME Journal of Turbomachinery*. 116 (1992): 113-123.

## 4.2.2.2 Enhanced Internal Cooling of Turbine Blades and Vanes

71. C.W. Park, S.C. Lau, R.T. Kukreja, "Heat/Mass Transfer in a Rotating Two-Pass Square Channel with Transverse Ribs," *AIAA Journal of Thermophysics and Heat Transfer* 12 (1998): 80-86; C.W. Park, C. Yoon, S.C. Lau, "Heat (Mass) Transfer in a Diagonally Oriented Rotating Two-Pass Channels with Rib-Roughened Walls," *ASME Journal of Heat Transfer* 122 (2000): 208-211.
72. B.V. Johnson, J.H. Wagner, G.D. Steuber, and F.C. Yeh, "Heat Transfer in Rotating Serpentine Passages with Selected Model Orientations for Smooth or Skewed Trip Walls," *ASME Journal of Turbomachinery* 116 (1994): 738-744.
73. J.A. Parsons, J.C. Han, and Y.M. Zhang, "Wall Heating Effect on Local Heat Transfer in a Rotating Two-Pass Square Channel with 90-Degree Rib Turbulators," *International Journal of Heat and Mass Transfer* 37 (1994): 1411-1420.
74. S. Dutta and J.C. Han, "Local Heat Transfer in Rotating Smooth and Ribbed Two-Pass Square Channels With Three Channel Orientations," *ASME Journal of Heat Transfer* 118 (1996): 578-584.
75. L. Al-Hadhrami and J.C. Han, "Effect of Rotation in Two-Pass Square Channels with Parallel and Crossed 45 angled Rib Turbulators," *International Journal of Heat and Mass Transfer* 46 (2003): 653-669.
76. J. Guidez, "Study of the Convective Heat Transfer in a Rotating Coolant Channel," *ASME Journal of Turbomachinery* 111(1989): 43-50.
77. C.Y. Soong, S.T. Lin, and G.J. Hwang, "An Experimental Study of Convective Heat Transfer in Radially Rotating Rectangular Ducts," *ASME Journal of Heat Transfer* 113 (1991): 604-611.
78. M.E. Taslim, L.A. Bondi, and D.M. Kercher, D.M., "An Experimental Investigation of Heat Transfer in an Orthogonally Rotating Channel Roughened with 45 Deg Criss-Cross Ribs on Two Opposite Walls," *ASME Journal of Turbomachinery* 113 (1991): 346-353.
79. G.M.S. Azad, J.M. Uddin, J.C. Han, H.K. Moon, and B. Glezer, "Heat Transfer in a Two-Pass Rectangular Rotating Channel with 45-Degree Angled Rib Turbulators," *ASME Journal of Turbomachinery* 124 (2001): 251-259; L. Al-Hadhrami, T.S. Griffith, and J.C. Han, "Heat Transfer in Two-Pass Rotating Rectangular Channels (AR=2) with Parallel and Crossed 45° V-shaped Rib Turbulators," *ASME Journal of Heat Transfer* 125 (2002): 232-242.
80. T.S. Griffith, L. Al-Hadhrami, and J.C. Han, "Heat Transfer in Rotating Rectangular Cooling Channels (AR=4) with Angled Ribs," *ASME Journal of Heat Transfer* 124 (2001): 617-625.
81. E. Lee, L.M. Wright, and J.C. Han, "Heat Transfer in Rotating Rectangular Channels (AR = 4:1) with V-Shaped and Angled Rib Turbulators with and without Gaps," ASME Paper No. GT-2003-38900 (2003).
82. L.M. Wright, W.L. Fu, and J.C. Han, "Thermal Performance of Angled, V-Shaped, and W-Shaped Rib Turbulators in Rotating Rectangular Cooling Channels (AR=4:1)," ASME Paper No. GT 2004-54073 (2004).
83. H.H. Cho, Y.Y. Kim, K.M. Kim, and D.H. Rhee, "Effects of Rib Arrangements and Rotation Speed on Heat Transfer in a Two-Pass Duct," ASME Paper No. GT 2003-38609 (2003).
84. P. Agarwal, S. Acharya, and D.E. Nikitopoulos, "Heat/Mass Transfer in 1:4 Rectangular Passages with Rotation," ASME Paper No. GT 2003-38615 (2003).
85. W.L. Fu, L.M. Wright, and J.C. Han, "Heat Transfer in Two-Pass Rotating Rectangular Channels (A=1:2 and AR=1:4) with Smooth Walls," *ASME Journal of Heat Transfer* 127 (2005): 209-356; W.L. Fu, L.M. Wright, and J.C. Han, "Heat Transfer in Two-Pass Rotating Rectangular Channels (AR=1:2 and AR=1:4) with 45° Angled Rib Turbulators," ASME Paper No. GT 2004-53261 (2004); W.L. Fu, L.M. Wright, and J.C. Han, "Buoyancy Effects on Heat Transfer in Five Different Aspect-Ratio Rectangular Channels with Smooth Walls and 45-Degree Ribbed Walls," ASME Paper No. GT 2005-68493 (2005).
86. R.J. Clifford, W.D. Morris, and S.P. Harasgama, "An Experimental Study of Local and Mean Heat Transfer in a Triangular-Sectioned Duct Rotating in the Orthogonal Mode," *ASME Journal of Engineering for Gas Turbines and Power* 106 (1984): 661-667.
87. S.P. Harasgama and W.D. Morris, "The Influence of Rotation on the Heat Transfer Characteristics of Circular, Triangular, and Square-Sectioned Coolant Passages of Gas Turbine Rotor Blades," *ASME Journal of Turbomachinery* 110 (1988): 44-50.
88. S. Dutta, J.C. Han, Y.M. Zhang, and C.P. Lee, "Local Heat Transfer in a Rotating Two-Pass Triangular Duct with Smooth Walls," *ASME Journal of Turbomachinery* 118 (1996): 435-443; S. Dutta, J.C. Han, and C.P. Lee, "Local Heat Transfer in a Rotating Two-Pass Ribbed Triangular Duct with Two Model Orientations," *International Journal of Heat and Mass Transfer* 39 (1996): 707-715.
89. L. Rathjen, D.K. Hennecke, S. Bock, S., and R. Kleinstuck, "Detailed Heat/Mass Transfer Distributions in a Rotating Two Pass Coolant Channel with Engine-Near Cross section and Smooth Walls," in Heat Transfer in Gas Turbine Systems, edited by Richard J. Goldstein, *Annals of the New York Academy of Sciences* 934 (2001): 432-439.
90. See note 95.
91. See note 81.
92. See note 85 (ASME Paper No. GT 2005-68493).
93. G. Su, H.C. Chen, J.C. Han, and D. Heidmann, "Computation of Flow and Heat Transfer in Two-Pass Rotating Rectangular Channels (AR=1:1, AR=1:2, AR=1:4) with 45-Deg Angled Ribs by a Reynolds Stress Turbulence Model," ASME Paper No. GT2004-53662 (2004).
94. See note 85.
95. Ibid.

96. Ibid.
97. C. Prakash and R. Zerkle, "Prediction of Turbulent Flow and Heat Transfer in a Radially Rotating Square Duct," *ASME Journal of Turbomachinery* 117 (1992): 255-261.
98. Y.L. Lin, T.I-P Shih, M.A. Stephens, and M.K. Chyu, "A Numerical Study of Flow and Heat Transfer in a Smooth and Ribbed U-Duct With and Without Rotation," *ASME Journal of Heat Transfer* 123 no. 2 (2001): 219-232.
99. H.C. Chen, Y.J. Jang, and J.C. Han, "Computation of Flow and Heat Transfer in Rotating Two-Pass Square Channels by a Reynolds Stress Model," *International Journal of Heat and Mass Transfer* 43 no. 9 (2000): 1603-1616; H.C. Chen, Y.J. Jang, and J.C. Han, "Near-Wall Second-Moment Closure for Rotating Multiple-Pass Cooling Channels," *AIAA Journal of Thermophysics and Heat Transfer* 14 no. 2 (2000): 201-209.
100. Y.J. Jang, H.C. Chen, and J.C. Han, "Flow and Heat Transfer in a Rotating Square Channel with 45-Degree Angled Ribs by Reynolds Stress Turbulence Model," *ASME Journal of Turbomachinery* 123 no. 1 (2001): 124-132.
101. M. Al-Qahtani, Y.J. Jang, H.C. Chen, and J.C. Han, "Prediction of Flow and Heat Transfer in Rotating Two-Pass Rectangular Channels with 45-Degree Rib Turbulators," *ASME Journal of Turbomachinery* 124 (April, 2002): 242-250.
102. G. Su, S. Tang, H.C. Chen, and J.C. Han, "Flow and Heat Transfer Computations in Rotating Rectangular Channels with V-Shaped Ribs," *AIAA Journal of Thermophysics and Heat Transfer* 18 no. 4 (2004): 534-547.
103. See note 101.
104. See note 93.
105. D.K. Lezius and J.P. Johnston, "Roll-Cell Instabilities in Rotating Laminar and Turbulent Channel Flows," *Journal of Fluid Mechanics* 77 (1976): 153-175.
106. M. Elfert, "The Effect of Rotation and Buoyancy on Flow Development in a Rotating Circular Coolant Channel," 2<sup>nd</sup> International Symposium on Engineering Turbulence Modeling and Measurements, May 31-June 2, 1993, Florence, Italy.
107. D.G.N. Tse and D.B. McGrath, "A Combined Experimental/Computational Study of Flow in Turbine Blade Cooling Passage. Part I: Experimental Study," ASME Paper No. 95-GT-355 (1995).
108. D.G.N. Tse and G.D. Steuber, "Flow in a Rotating Square Serpentine Coolant Passage with Skewed Trips," ASME Paper No. 97-GT-529 (1997).
109. S.C. Cheah, H. Iacovides, D.C. Jackson, H. Ji, and B.E. Launder, "LDA Investigation of the Flow Development through Rotating U-Ducts," *ASME Journal of Turbomachinery* 118 (1996): 590-595.
110. J.P. Bons and J.L. Kerrebrock, "Complementary Velocity and Heat Transfer Measurements in a Rotating Cooling Passage with Smooth Walls," ASME Paper No. 98-GT-464 (1998).
111. J. Schabacker, A. Bolcs, and B.V. Johnson, "PIV Investigation of the Flow Characteristics in an Internal Coolant Passage with 45° Rib Arrangement," ASME Paper No. GT 99-120 (1999); D. Chanteloup, Y. Yuaneda, and A. Bolcs, "Combined 3D Flow and Heat Transfer Measurements in a 2-pass Internal Coolant Passage of Gas Turbine Airfoil," ASME Paper No. GT 2002-30214 (2002).
112. S.Y. Son, K.D. Kihm, and J.C. Han, "PIV Flow Measurements for Heat Transfer Characterization in Two-Pass Square Channels with Smooth and 90-degree Ribbed Walls," *International Journal of Heat and Mass Transfer* 45 no. 24 (2002): 4809-4822.
113. T.M. Liou and C.C. Chen, "LDV Study of Developing Flows through a Smooth Duct with a 180 Deg Straight-Corner Turn," *ASME Journal of Turbomachinery* 121 (1999): 167-174.
114. T.M. Liou, M.Y. Chen, and M.H. Tsai, "Fluid Flow and Heat Transfer in a Rotating Two-Pass Square Duct with In-Line 90° Ribs," ASME Paper No. GT 2001-0185 (2001).
115. T.M. Liou, M.Y. Chen, and Y.M. Wang, "Heat Transfer, Fluid Flow, and Pressure Measurements inside a Rotating Duct with Detached 90° Ribs," ASME Paper No. GT 2002-30201 (2002).
116. Liou, T. M., and Dai, G. Y., 2003, "Pressure and Flow Characteristics in a Rotating Two-Pass Square Duct with 45 Deg Angled Ribs," ASME Paper No. GT 2003-38346.
117. T.M. Liou, Y.S. Hwang, and Y.C. Li, "Flowfield and Pressure Measurements in a Rotating Two-Pass Duct with Staggered Rounded Ribs Skewed 45° to the Flow," ASME Paper No. GT 2004-53173 (2004).
118. See notes 116 and 117.
119. A.H. Epstein, J.L. Kerrebrock, J.J. Koo, and U.Z. Preiser, "Rotational Effects on Impingement Cooling," GTL Report No. 184 (1985).
120. C.H. Mattern and D.K. Hennecke, "The Influence of Rotation on Impingement Cooling," ASME Paper No. 96-GT-161 (1996).
121. B. Glezer, H.K. Moon, J. Kerrebrock, J. Bons, and G. Guenette, "Heat Transfer in a Rotating Radial Channel with Swirling Internal Flow," ASME Paper No. 98-GT-214 (1998).
122. J.A. Parsons, J.C. Han, and C.P. Lee, "Rotation Effect on Jet Impingement Heat Transfer in Smooth Rectangular Channels with Four Heated Walls and Radially Outward Crossflow," *ASME Journal of Turbomachinery* 120 (1998): 79-85.
123. K.V. Akella and J.C. Han, "Impingement Cooling in Rotating Two-Pass Rectangular Channels," *AIAA Journal of Thermophysics and Heat Transfer* 12 no. 4 (1998): 582-588.

## 4.2.2.2 Enhanced Internal Cooling of Turbine Blades and Vanes

124. J.A. Parsons and J.C. Han, "Rotation Effect on Jet Impingement Heat Transfer in Smooth Rectangular Channels with Heated Target Walls and Film Coolant Extraction," ASME Paper No. 96-WA/HT-9 (1996).
125. K.V. Akella and J.C. Han, "Impingement Cooling in Rotating Two-Pass Rectangular Channels with Ribbed Walls," *AIAA Journal of Thermophysics and Heat Transfer* 13 no. 3 (1999): 364-371.
126. J.A. Parsons, J.C. Han, and C.P. Lee, "Rotation Effect on Jet Impingement Heat Transfer in Smooth Rectangular Channels with Four Heated Walls and Film Coolant Extraction," ASME Paper No. GT-2003-28905 (2003).
127. F.T. Willett and A.E. Bergles, "Heat Transfer in Rotating Narrow Rectangular Ducts with Heated Sides Oriented at 60-Degree to the R-Z Plane," ASME Paper No. 2000-GT-224 (2000); F.T. Willett and A.E. Bergles, "Heat Transfer in Rotating Narrow Rectangular Pin-Fin Ducts," *Experimental Thermal and Fluid Science* 25 (2002): 573-582.
128. L.M. Wright, E. Lee, and J.C. Han, "Effect of Rotation on Heat Transfer in Narrow Rectangular Cooling Channels (AR = 8:1 and 4:1) with Pin-Fins," ASME Paper No. GT 2003-38340 (2003).
129. F. Zhou and S. Acharya, "Mass/Heat Transfer in Dimpled Two-Pass Coolant Passages with Rotation," *Heat Transfer in Gas Turbine Systems*, ed., R. J. Goldstein, Ann. N. Y. Acad. Sci., 934 (2001): 424-431.
130. T.S. Griffith, L. Al-Hadhrami, and J.C. Han, "Heat Transfer in Rotating Rectangular Cooling Channels (AR = 4) with Dimples," *ASME Journal of Turbomachinery* 125 (2003): 555-563.





# BIOGRAPHY

## 4.2.2 Enhanced Internal Cooling of Turbine Blades and Vanes



### **Je-Chin Han**

Turbine Heat Transfer Laboratory  
Department of Mechanical Engineering  
Texas A&M University  
College Station, Texas 77843-3123

phone: (979) 845-3738  
email: [jc-han@tamu.edu](mailto:jc-han@tamu.edu)

Dr. Han is presently the Marcus Easterling Endowed Chair Professor at Texas A & M University. He has been working on many turbine blade cooling projects since 1980, including innovative cooling concepts, rotor coolant passage heat transfer, unsteady high turbulence effects on blade film cooling and turbine edge cooling (leading edge, trailing edge, blade tip, and end-wall regions). This research has been on both aircraft engines and industrial gas turbine applications funded by NASA- Glenn, GE - aircraft engines, DOE - AGTSR + UTSR, and Siemens Westinghouse. He is the co-author of more than 150 refereed journal papers and one book in gas turbine heat transfer and cooling technology. He has been doing research on gas turbine blade cooling for more than 25 years.



## **Lesley M. Wright**

Turbine Heat Transfer Laboratory  
Department of Mechanical  
Engineering  
Texas A&M University  
College Station, Texas 77843-3123

phone: (979) 845-1767  
email: [lesleywright@neo.tamu.edu](mailto:lesleywright@neo.tamu.edu)

Lesley Wright is a Ph.D. candidate in the Department of Mechanical Engineering at Texas A&M University. She joined the Turbine Heat Transfer Laboratory in September of 2001 after obtaining her B.S. in Engineering from Arkansas State University. While experimentally investigating the effect of rotation on internal gas turbine blade heat transfer, she earned her M.S. in Mechanical Engineering from Texas A&M in May of 2003. Lesley continues to study both internal and external turbine blade heat transfer; in addition, she is considering new experimental methods and their application to better understand gas turbine heat transfer and cooling techniques.